Title: Testosterone-Induced Metabolic Changes in Seminal Vesicle Epithelium Modify Seminal Plasma Components with Potential to Improve Sperm Motility

Authors: Takahiro Yamanaka[1], Zimo Xiao[1], Natsumi Tsujita[1], Mahmoud Awad[1,2], Takashi Umehara[1], Masayuki Shimada[1,3*]

Affiliations:

[1] Graduate School of Integrated Sciences for Life, Hiroshima University; Higashihiroshima, Hiroshima, Japan

[2] Department of Histology, Faculty of Veterinary Medicine, South Valley University; Qena, Egypt

[3] Graduate School of Innovation and Practice for Smart Society, Hiroshima University; Higashihiroshima, Hiroshima, Japan

*Corresponding author. Masayuki Shimada, Ph.D. E-mail: mashimad@hiroshima-u.ac.jp, Tel/Fax: (+81)-824-24-7899

One Sentence Summary: Testosterone promotes the conversion of glucose to fatty acid by increasing the expression of ACLY in seminal vesicle epithelial cells, thereby regulating the seminal plasma components.

Abstract:

Male factors account for almost half of the causes of infertility. In rodents and humans, most of the components of semen are supplied by the seminal vesicles, and they support male reproductive ability, but there are many unknown details. In this study, the metabolic changes in the seminal vesicle epithelial cells were focused on, and the mechanisms by which testosterone affected the seminal plasma composition were investigated. A factor improving the linear motility of sperm was secreted from the seminal vesicles, and it was produced in an androgen-dependent manner. Bioassays, gene expression, and flux analysis studies demonstrated that testosterone promotes glucose uptake in seminal vesicle epithelial cells via GLUT4, resulting in fatty acid synthesis. ACLY was a critical factor in this metabolic change, which produced fatty acid, especially oleic acid. In conclusion, the critical role of testosterone-induced metabolic changes in

the seminal vesicles is to ensure the synthesis of fatty acid. These findings suggest that testosterone-dependent lipid remodeling may contribute to sperm straight-line motility, and further functional verification is required.

Main Text:

INTRODUCTION

Infertility is defined by the World Health Organization (WHO) as the failure to conceive within 12 months despite contraceptive-free sexual intercourse. Its prevalence has increased over the decades and is observed in 17.5% of couples worldwide *(1)*. The male partner is thought to be solely or in combination responsible for 50% of infertility cases, and the male factor in the etiology of infertility is highly recognized. Male fertility depends largely on the quality of semen composed of sperm and seminal plasma and decreases with aging*(2–4)*.

Sperm that have completed spermatogenesis in the testis acquire the potential to fertilize during maturation in the epididymis *(5–7)*. The physiological change of sperm during fertilization process are collectively referred to as "capacitation". This change is characterized by large-amplitude flagellar beating (called hyperactivation) and developing the capacity to undergo the acrosome reaction, and can be induced by culturing sperm collected from the epididymis in a medium containing bicarbonate and cholesterol acceptors *(8, 9)*. However, once capacitation is complete, sperm cannot maintain this state for a long time. Therefore, even if epididymal sperm that have not been exposed to seminal plasma are artificially inseminated into the cervix or uterus, the fertilization rate remains low *(10–12)*. This is because, *in vivo*, during ejaculation, exposure of epididymal sperm to seminal plasma masks the unintended capacitation as they pass through the female reproductive tract and ensures fertilization of sperm that reaches the oviduct *(13)*. In other words, seminal plasma plays an important role in fine-tuning the timing of sperm capacitation and in maintaining the sustained sperm motility required to reach the oviduct.

Seminal plasma is mainly produced in the seminal vesicles (approximately 65-75%), with approximately 20-30% produced by the prostate, and small amounts secreted by the bulbourethral and urethral glands *(14)*. The mixing of seminal fluid with accessory reproductive gland fluid during ejaculation causes semen to clot and liquefy in humans and causes vaginal plug formation in rodents. Vaginal plugs not only inhibit continuous mating but also play a role in maintaining sperm in the uterus and ensuring male fertility *(13)*. TGFβ, a component of seminal plasma, increases antigen-specific Treg cells in the uterus of mice and humans, which induces immune tolerance, resulting in pregnancy *(15, 16)*. Furthermore, SVS2, secreted from the seminal vesicle, is also known to be required for sperm to escape attack by the female immune system in the uterus

64 *(17)*. In addition, seminal plasma contains various biochemical components that support sperm
65 metabolism, including lipids and organic acids. Differences in the relative size of the accessory
66 reproductive glands reflect differences in the seminal plasma composition. Accordingly, there are
67 considerable differences in the properties of seminal plasma among animal species. Specifically,
68 Rosecrans et al. *(18)* found significant differences in the levels of most biochemical components
69 in seminal plasma compared to those in blood, with specific factors like fructose being rarely
70 detected in blood but abundant in seminal plasma. Our previous studies *(19–21)* documented that
71 seminal plasma also contains creatine and fatty acids taken up by sperm within minutes. These
72 substances play crucial roles in regulating sperm metabolic pathways and enhancing sperm
73 motility. These observations indicate that seminal plasma not only alters the female immune
74 system to protect sperm but also directly influences sperm metabolic pathways, facilitating the
75 transformation of sperm capable of *in vivo* fertilization.

76 Several specific factors produced by the male accessory glands that contribute to seminal
77 plasma and impact male fertility have been elucidated. For example, surgical removal of seminal
78 vesicles in male mice and rats was associated with infertility *(17, 22, 23)*. The observations that
79 fructose *(24)* and citrate*(25)* concentrations in seminal plasma of control mice and rats are higher
80 than in castrated animals suggest that the specific metabolism of the accessory glands might be
81 affected by testosterone derived from the testes, which activate intracellular androgen receptors
82 (AR; NR3C4) required for gene regulation of transcription. AR-deficient mice have been found
83 to be infertile *(26)*, and long-term administration of androgen receptor antagonists, like flutamide,
84 abolished male fertility *(27, 28)*. AR-deficient mice and transcriptome analyses have identified
85 specific targets of AR *(29, 30)*. In both mice and humans, androgen levels decrease with aging,
86 and their concentrations have been reported to cause a decrease in male fertility, especially
87 ejaculated sperm motility. In addition to impairments in spermatogenesis, a decline in androgen
88 levels may also disrupt the metabolic functions of the accessory glands and alter the composition
89 of seminal plasma. Therefore, the intricate interplay between testosterone and seminal plasma
90 synthesis in the accessory glands requires further investigation.

91 In this study, various bioassays were done to identify which accessory glands are essential for
92 sperm fertility. Subsequently, comparative *in vivo* and *in vitro* analyses were performed using a
93 hypoandrogenic model. In addition, biochemical and molecular techniques such as RNA-seq, flux

94 analysis, mass spectrometry, and knockdown experiments were employed. These analyses
95 revealed that testosterone promotes the synthesis of oleic acid in seminal vesicle epithelial cells
96 and its secretion into seminal plasma.
97
98 **RESULTS**
99 **The effect of androgen-dependent changes in mouse seminal vesicle secretions on the**
100 **linear motility of sperm**
101 A direct comparison was conducted to clarify the effects of secretions from the prostate and
102 seminal vesicles on the motility parameters of epididymal sperm. Since it is difficult to collect the
103 ejaculated semen of mice, a pseudo-seminal plasma was prepared using seminal vesicle secretions
104 and homogenized prostate tissue (Fig.1A, Supplemental Fig.1A). When seminal vesicle
105 secretions were added to the HTF medium, the sperm motility, progressive motile, the straight
106 line velocity (VSL), and the percentage of linearity (LIN) values increased significantly compared
107 to when only prostate extract was used. However, the curvi-linear velocity (VCL) did not change
108 (Fig.1B-F). Meanwhile, the secretions from the prostate and seminal vesicles did not affect the
109 viscosity of the medium (Fig.1G). These results indicate that sperm exposure to seminal plasma
110 factors significantly improved sperm linear motility (high VSL and LIN).
111 Androgens regulate the functions of seminal vesicles. Therefore, to elucidate whether the
112 seminal vesicle factors, which enhance sperm linear motility, are synthesized in an androgen-
113 dependent manner, bioassays were performed using seminal vesicle secretions collected from
114 control mice or mice treated daily for 7 consecutive days with flutamide, an androgen receptor
115 antagonist (Fig. 1H, Supplemental Fig.1B). The results showed that Motile, Progressive motile,
116 LIN, and VSL were significantly reduced in the sperm cultured in seminal vesicle secretions from
117 flutamide-treated (Flutamide) compared to the sperm cultured in seminal vesicle secretions from
118 controls (Ctrl) (Fig.1I-L). The reduction of VSL, Motile, and Progressive motile were also
119 significantly lower in the sperm treated with seminal vesicle secretions from over 12 months old
120 mice that showed low circulating testosterone levels as compared with the sperm treated with
121 seminal vesicle secretions from young adult mice (3 months old mice) (Supplemental Fig.2A,B).
122 Furthermore, JC-1 staining to measure mitochondrial membrane potential, which is important for
123 sperm linear motility, showed a significantly lower percentage of high mitochondrial membrane

124 potential in sperm treated with the secretions of seminal vesicles from flutamide-treated mice and
125 over 12 months old mice (Fig.1M, Supplemental Fig.1C,D, Supplemental Fig.2C). Since
126 flutamide treatment and aging also affect spermatogenesis and sperm motility, it should be noted
127 that epididymal sperm donors differ from seminal vesicle donors (Fig. 1H). Due to the strong
128 effect of the decapacitation factor, it was found that seminal vesicle fluid, regardless of the
129 presence or absence of androgens, reduces the fertilization rate in *in vitro* fertilization
130 (Supplemental Figure 1E). The baseline information for the epididymal sperm used in the
131 experiment showed that the sperm were normal (Supplemental Fig.1A). These results indicated
132 that androgen-dependent changes in seminal vesicle functions alter the levels/activity of seminal
133 vesicle secretion factors, which regulate sperm linear motility. The changes in seminal vesicle
134 functions were also induced by aging.
135

136 **Testosterone-androgen receptor activity suppresses the proliferation of seminal vesicle epithelial**
137 **cells**

138 To understand the difference between seminal vesicles that secrete factors for enhancing sperm
139 linear motility and those that are impaired in this function, we performed histological analysis of
140 seminal vesicles recovered from mice treated and non-treated with flutamide. In control mice, the
141 seminal vesicle epithelial cells were in a single layer, and androgen receptors were localized in the
142 nuclei of seminal vesicle epithelial cells (Fig.2A). However, in mice treated with continuous
143 administration of flutamide, seminal vesicle epithelial cells were multilayered, and the strong
144 accumulation of androgen receptors in nucleus was not observed (Fig.2A). To investigate the cause
145 of this multilayering of cells, we performed Ki67 staining, a marker of cell proliferation, and
146 apoptosis detection by TUNEL staining (Fig.2B). The results showed that the percentage of Ki67-
147 positive cells increased significantly after treatment with flutamide, but the percentage of TUNEL-
148 positive cells did not change, suggesting that the testosterone-androgen receptor pathway is
149 responsible for the inhibition of proliferation of seminal vesicle epithelial cells (Fig.2C). These
150 changes of abnormal morphology and high proliferation activity were also observed in seminal
151 vesicle of more than 12 months old mice that showed the low level of testosterone in serum
152 (Supplemental Figure 2D-F). Therefore, seminal vesicle epithelial cells were collected and cultured

153 in primary culture, as shown in Fig. 2D. The changes in cell number were counted, and the cell
154 cycle was analyzed by flow cytometry. When cultured without testosterone (c), the number of
155 seminal vesicle epithelial cells increased time-dependent manner. However, the addition of
156 testosterone significantly decreased the number of seminal vesicle epithelial cells during the 8-day
157 culture period in a concentration-dependent manner (Fig.2E). Flow cytometry on day 7 revealed a
158 significant increase in the proportion of cells in the G0/G1 phase and a corresponding decrease in
159 the G2/M phase. The G2/M phase was significantly decreased by the addition of testosterone (Fig.
160 2F,G). These results indicate that the testosterone-androgen receptor pathway inhibits seminal
161 vesicle epithelial cells in cell division.

162

163 **Testosterone alters metabolic gene expression in seminal vesicle epithelial cells**

164 To better understand the roles of testosterone in suppressing the proliferation of seminal vesicle
165 epithelial cells, RNA sequencing was done using the epithelial cells cultured with or without
166 testosterone. DEG (Differential Expressed Genes) analysis revealed that a total of 23,459 genes
167 were identified, including 997 upregulated genes and 3463 downregulated genes in seminal
168 vesicle epithelial cells by testosterone relative to control (Fig.3A). Genes largely upregulated
169 by testosterone included those already reported in seminal vesicles *(17, 22, 31)*, such as the
170 Seminal Vesicle Secretion (*Svs*) family (*Svs1~6*), *Pate4*, *Spinkl*, *Ceacam10*, and *Sva* (Fig.3B,C).
171 Therefore, the primary culture of seminal vesicle epithelial cells used in this experiment was
172 considered to maintain the characteristics of seminal vesicle epithelial cells *in vivo*. Many genes
173 were downregulated by testosterone, and those with a high rate of variation included collagen
174 synthase and *Mmp2*, which are involved in extracellular matrix formation (Fig.3C). However,
175 KEGG analysis, rather than individual genes, was used to predict functions altered by
176 testosterone. It was found that the expression of genes involved in the metabolic pathway was
177 the most highly affected by testosterone (Fig.3D). Because there is a close relationship between
178 cell proliferation and metabolic activity and between metabolic substrates in seminal plasma and
179 sperm motility, we hypothesized that testosterone induced changes in seminal vesicle epithelial
180 cell metabolism alter the components of seminal plasma to mediate the enhancement of sperm
181 motility.

182

183 **Testosterone shifts the metabolic flux of seminal vesicle epithelial cells**

184 In the presence of testosterone, the addition of glucose significantly activated the extracellular
185 acidification rate (ECAR) normalized by the total number of live cells compared to that in
186 epithelial cells cultured without testosterone (Fig.4A-C). These data indicate that testosterone
187 enhances glucose utilization. This leads to the interpretation that testosterone increases the flow
188 of glycolysis by increasing glucose uptake and alters metabolic flux distribution. To determine
189 the metabolic fate of glycolytic end products, seminal vesicle epithelial cells were cultured with
190 and without testosterone. Subsequently, the concentrations of pyruvate and lactate in the culture
191 supernatant normalized by the total number of live cells were measured. The addition of
192 testosterone significantly decreased the pyruvate concentration; however, the lactate
193 concentration did not change significantly (Fig.4D,E). We therefore examined cellular energy
194 metabolism with a flux analyzer, anticipating that testosterone would elevate glycolytic flux, thereby
195 producing more pyruvate from phosphoenolpyruvate. Because extracellular pyruvate levels
196 simultaneously declined, we inferred that the cells had an increased pyruvate demand and, at that time,
197 hypothesized that the excess pyruvate would enter the mitochondria to support enhanced oxidative
198 metabolism. Unexpectedly, when measuring mitochondrial respiratory metabolism normalized
199 by the total number of live cells with the flux analyzer, the basal respiratory rate (the electron
200 transport chain activity) was significantly decreased by testosterone (Fig.4F-J). Oligomycin-
201 sensitive respiration was also significantly suppressed by exposure to testosterone. Furthermore,
202 the FCCP uncoupled respiration and spare respiration capacity were also significantly decreased
203 in response to testosterone treatment. Overall, these data indicate that testosterone promotes the
204 redistribution of metabolic flux. In other words, testosterone increased glycolysis in seminal
205 vesicle epithelial cells while decreasing mitochondrial respiration. To determine whether these
206 changes were accompanied by changes in gene expression of specific metabolic-related enzymes,
207 we analyzed gene expression levels.

208

209 **Testosterone causes changes in the expression of genes encoding enzymes involved in glucose**
210 **catabolism and anabolism**

211 The expression of genes involved in glucose catabolism and anabolism in the *in vitro* culture
212 system of seminal vesicle epithelial cells was analyzed by qPCR (Fig.5). The gene expression of
213 glucose transporter (*Glut*) and enzymes involved in the glycolytic pathway was not significantly
214 affected by testosterone, consistent with the results of metabolic flux analysis, which showed that
215 the glycolytic pathway was not enhanced despite the activation of the glycolysis. Furthermore,
216 testosterone did not significantly affect the expression of genes encoding enzymes involved in the
217 TCA cycle in mitochondria. However, the expression of enzymes involved in the electron
218 transport chain was significantly decreased. Interestingly, testosterone significantly increased the
219 expression of *Acly*, which encodes a cytoplasmic enzyme that converts citrate transported from
220 the TCA cycle into acetyl-CoA, a substrate that is essential for fatty acid synthesis. Although
221 *Hmgcr*, which encodes the rate-limiting enzyme involved in cholesterol synthesis, was unchanged,
222 the expression of *Acc*, which encodes the rate-limiting enzyme for fatty acid synthesis, was
223 significantly upregulated by testosterone. These characteristic testosterone-induced changes in
224 gene expression observed in cultured cells were also detected by ACLY immunostaining of *in*
225 *vivo* seminal vesicle samples (Supplemental Figure 3). Specifically, the expression of genes
226 encoding a group of enzymes of the electron transport chain (*mtNd6*) was significantly
227 upregulated by continuous flutamide administration *in vivo*, whereas the gene expression of *Acly*
228 and *Acc* was significantly decreased by flutamide administration (Supplemental Figure 3B).
229 Immunostaining results showed that ACLY was detected specifically in seminal vesicle epithelial
230 cells, and their staining appeared to be reduced by flutamide treatment. The lower level of ACLY
231 was also observed in seminal vesicle epithelial cells of over 12 months old mice (Supplemental
232 Figure 3C).
233
234 **Mechanism of testosterone-induced enhancement of glucose uptake and, thereby, fatty acid**
235 **synthesis**
236 Since it is known that testosterone regulates the intracellular localization of GLUT4, we
237 focused on the intracellular localization of GLUT4 and its glucose uptake capacity *(32, 33)*. The
238 effect of testosterone on glucose uptake in seminal vesicle epithelial cells was analyzed using
239 fluorescence-labeled glucose. As expected from the results of flux metabolic analyses,
240 testosterone treatment significantly increased glucose uptake (Fig.6A). Indinavir, a functional

241 inhibitor of GLUT4, significantly suppressed glucose uptake and significantly decreased fatty
242 acid synthesis (the amount of fatty acids accumulated in the cell), which was increased by
243 testosterone (Fig.6A,B).
244 Furthermore, immunostaining analysis of the localization of GLUT4 in seminal vesicles
245 revealed that GLUT4 was translocated outside the nucleus of seminal vesicle epithelial cells
246 under the presence of testosterone (Fig.6C). These data suggest that GLUT4 was partially
247 localized at the plasma membrane and contributed to glucose uptake. In contrast, in seminal
248 vesicles from mice continuously treated with flutamide, no strong signal was detected at the
249 presumed location of GLUT4 near the plasma membrane of seminal vesicle epithelial cells, even
250 though the protein expression level was not affected (Fig.6C,D). The same characteristics were
251 observed in aged mice.
252 Qualitative and quantitative analysis of the fatty acids synthesis was performed by GC-MS.
253 In seminal vesicles, C16:0, C18:0, and C18:1 were detected, in which C18:1 was decreased to
254 an undetectable level in seminal vesicles of mice treated with the flutamide (Supplemental
255 Figure 4A). In the cultured seminal vesicle epithelial cells, C18:1, oleic acid, was significantly
256 increased by the addition of testosterone as observed in the seminal vesicle (Fig.6E). The
257 expression of *Elovl6* encoding ELOVL6, which desaturates C18:0 saturated fatty acids to C18:1,
258 was significantly up-regulated by testosterone (Fig.6F,G). The testosterone-induced change was
259 also detected in *in vivo* samples (seminal vesicle), where the expression of *Elovl6* was decreased
260 by the flutamide treatment (Supplemental Figure 4B).
261 In order to examine whether these lipids are the factors that induces sperm linear motility, we
262 examined whether or not the addition of lipid mixture changed in sperm motility pattern
263 (Supplemental Figure 5). The lipid mixture did not affect sperm motility at any concentration
264 compared to the control (LM 0%). However, VSL was significantly increased in sperm with 1%
265 lipid mixture added.
266
267 **ACLY expression is upregulated by testosterone and is essential for the metabolic shift that**
268 **is associated with increased linear motility**
269 ACLY is upregulated in seminal vesicle epithelial cells as a factor that enables the utilization
270 of citrate from the TCA cycle for fatty acid synthesis outside the mitochondria. Therefore, we

271 performed shRNA knockdown experiments on ACLY to clarify the impact of ACLY on the
272 cellular metabolic shift. The addition of testosterone significantly increased the amount of ACLY
273 protein in seminal vesicle epithelial cells (Fig.7A,B). Viral infection with shRNAs encoding
274 *Acly*-targeted shRNAs markedly decreased the amount of ACLY (Fig.7C). When ACLY was
275 knocked down using shRNA, the proliferation arrest caused by testosterone was released, and
276 the cells began to proliferate again (Fig.7D). This knockdown of ACLY increased the oxygen
277 consumption of seminal vesicle epithelial cells in the control and testosterone-treated group
278 (Fig.7E,F). Thus, ACLY expression is associated with mitochondrial metabolic pathway activity
279 in seminal vesicle epithelial cells. Furthermore, the knockdown of ACLY also significantly
280 suppressed testosterone-induced fatty acid synthesis in seminal vesicle epithelial cells (Fig.7G).
281 According to the GC-MS quantification results, the amount of fatty acids secreted into the
282 culture medium was also reduced by ACLY knockdown. In particular, the enhancement of oleic
283 acid secretion by testosterone was inhibited by ACLY knockdown (Fig.7H-J). Supernatants from
284 epithelial cells of the testosterone-added group induced motility and linear motility (Highest
285 VSL and LIN; Fig.7K-N). However, the knockdown of ACLY significantly reduced the effects
286 of the culture supernatant on sperm motility and LIN (Fig.7K-N). These results found that cell
287 proliferation stops when a metabolic shift mediated by ACLY occurs, and glucose is reallocated
288 to fatty acid synthesis. Fatty acid synthesis is an important function of the seminal vesicles, and
289 it was found that when testosterone is present, fatty acid synthesis enhancement and cell
290 proliferation stop simultaneously. However, it is not known what effects occur when cell
291 proliferation stops.
292
293 **This characteristic metabolic mechanism induced by testosterone is also observed in**
294 **human seminal vesicle epithelial cells**
295 To determine whether these findings in mice could be applied to humans, the commercially
296 available human seminal vesicle epithelial cells were used for following studies (Fig.8A). The
297 growth curves showed that cell proliferation was inhibited by 100 ng/mL of testosterone
298 compared to the control; a pattern similar to that observed in murine seminal vesicle epithelial
299 cells (Fig.8B). The characteristics of metabolic activity of human seminal vesicle epithelial cells
300 were also similar to those of mice, with testosterone significantly enhancing the ECAR response

301 (Fig.8C-E), but significantly reducing the capacity for oxygen consumption in mitochondria
302 (Fig.8F-H). Moreover, fluorescent-glucose uptake was increased by testosterone and decreased
303 by the inhibitor of GLUT4 function (Fig.8I). Additionally, while testosterone also significantly
304 increased fatty acid synthesis, this increase was completely abolished by the GLUT4 inhibitor
305 (Fig.8J). According to the quantitative results obtained using GC-MS, the amount of fatty acids
306 secreted into the culture medium also decreased due to the inhibition of GLUT4 by indinavir. In
307 particular, it was shown that oleic acid secretion is completely dependent on glucose via GLUT4
308 (Fig.8K-M).
309

310 **DISCUSSION**

311 Seminal plasma has a variety of functions, including sperm transport, nutritional support,
312 interactions with the female reproductive tract, and especially the regulation of its relationship
313 with the female immune system. Mammalian seminal plasma is secreted mainly from the
314 seminal vesicle and is rich in cytokines, prostaglandins, and SVS family members *(34)*. For this
315 reason, recent studies have focused on the immunomodulatory function of seminal plasma in the
316 female reproductive tract. On the other hand, fructose and lipids in seminal plasma are the major
317 energy sources for sperm *(35)*. However, although metabolomic analyses of seminal plasma have
318 shown that metabolic substrates are present at higher concentrations in seminal plasma than in
319 blood *(18, 24, 25)*, how these substrates are synthesized and specifically how they alter sperm
320 motility has not been determined. Moreover, though the motility of ejaculated spermatozoa is
321 known to decrease with aging, few reports have revealed age-related changes in the seminal
322 vesicles, which are responsible for seminal plasma synthesis.

323 In this study, we focused on the reproductive organs that synthesize seminal vesicle secretion
324 as target organs for testosterone and found that factors formed by testosterone-dependent
325 metabolic changes in seminal vesicles activate sperm mitochondria and enhance their linear
326 motility. Testosterone is known to activate intracellular ARs and alter intracellular metabolic
327 pathways in skeletal muscle *(36)*, prostate cells *(37)* and cardiomyocytes *(33)*. ARs are known
328 to directly regulate the expression of glycolytic and lipid metabolic genes *(33, 38, 39)*. In the
329 present study, the nuclear localization of AR in seminal vesicle epithelial cells (i.e., functioning
330 as a transcription factor) and the activation of the glycolytic system by testosterone were similar

331 to those in the above cell types. In seminal vesicle epithelial cells, an increased trend in the
332 expression of *Glut3* and an enhancement of GLUT4 function were observed in a testosterone-
333 dependent manner. Such effects of testosterone on glucose metabolism have also been reported
334 in skeletal muscle, liver, and adipose tissue, where testosterone leads to the phosphorylation of
335 GLUT4 and enhances its translocation to the plasma membrane *(40, 41)*. This is consistent with
336 the results of our metabolic flux analyses, which show that testosterone increases the rate of
337 glycolysis in seminal vesicle epithelial cells by increasing glucose uptake. We further confirmed
338 that GLUT4 is the transporter that mediates this glucose uptake using indinavir, a GLUT4-
339 specific inhibitor.

340 This study suggests that fatty acid synthesis is an important function of the seminal vesicles,
341 which provide an environment where the ejaculated sperm can carry out active metabolism. The
342 shift to fatty acid synthesis was consistent with the cessation of cell proliferation in the presence
343 of testosterone. This mechanism could prevent the seminal vesicles from excessively consuming
344 the substrates necessary for sperm motility. Manipulation of ACLY expression in mouse
345 myoblasts and embryonic stem cells has been shown to alter the TCA cycle into a "non-normal
346 cycle" *(42)*. One advantage of the non-normal TCA cycle is its ability to retain carbon instead of
347 combusting it and to regenerate the cytosolic NAD+ needed to maintain glycolysis *(42, 43)*. It
348 suggests that ACLY, activated by testosterone, may suppress proliferation by skipping several
349 steps in the mitochondrial TCA cycle and minimizing ATP production associated with aerobic
350 respiration in seminal vesicle epithelial cells.

351 Testosterone has been reported to cause hypertrophy of cardiac myocytes *(44, 45)*. Cell
352 hypertrophy is partly due to the accumulation of fatty acids in the cytoplasm, which causes
353 significant damage to cellular functions *(46, 47)*. On the other hand, normal cell hypertrophy,
354 especially in myofibers, involves the activation of signaling molecules such as Myc, hypoxia-
355 inducible factor, and Pi3k-Akt-mTor, which regulate metabolic reprogramming in cancer by
356 increasing glucose uptake in the presence of oxygen *(48–50)*. In the present study, induction of
357 ACLY expression by testosterone not only decreased cycling in the TCA cycle, but also promoted
358 glucose assimilation, which played an important role in fatty acid synthesis. Thus, in tissues
359 where fatty acid synthesis is promoted, either β-oxidation-dependent ATP production in
360 mitochondria or the secretion of fatty acids occurs to maintain cellular function *(51–53)*

361 providing evidence to explain why the presence of fatty acids in the cell has no adverse effect.
362 In accessory reproductive glands, such as the prostate and seminal vesicles, the glucose uptake
363 is activated in a testosterone dependent. However, mitochondrial respiration is not enhanced,
364 cell proliferation is not induced, and the metabolites are used as a substrate for sperm motility.
365 This may be because, in the prostate, pyruvate synthesized by the glycolytic system in response
366 to testosterone is converted to acetyl CoA, which is then converted to citrate in the TCA cycle,
367 citrate is released as the main component of seminal plasma *(37)*.

368 The testosterone-dependent growth of cancerous prostate epithelial cells may be due to genetic
369 mutations, such as elevated expression of the gene encoding aconitase, which converts citrate to
370 isocitrate, which blocks the TCA cycle and inhibits citrate secretion *(54)*. On the other hand, in
371 the analysis of seminal vesicle epithelial cells, testosterone treatment induced the expression of
372 *Acc*, which encodes the rate-limiting enzyme for fatty acid synthesis, and *Elovl6*, which
373 desaturates to oleic acid, significantly increasing total saturated fatty acid and oleic acid content.
374 Therefore, testosterone promotes glucose conversion into fatty acids, especially oleic acid, in
375 seminal vesicle epithelial cells. Although there is a commonality in the activation of the
376 glycolytic system testosterone target tissues, the different expression patterns of genes involved
377 in metabolism in mitochondria may exert their specific functions in each tissue. In addition to
378 genes involved in fatty acid synthesis such as *Fasn* and *Elovl6*, *Acly* is also encoded in a region
379 in close proximity to human chromosome 17 and mouse chromosome 11, suggesting that in
380 seminal vesicle epithelial cells, this region is targeted to promote gene expression. The co-
381 regulation of these genes in seminal vesicle epithelial cells leads to synthesizing the fatty acids.

382 Decreased testosterone synthesis in the testes is a phenomenon observed with aging associated
383 with decreased spermatogenesis*(55)*. However, the probability of obtaining sperm without ICSI
384 or IVF is extremely low, despite the presence of sufficient numbers of sperm with normal-
385 morphology *(56–58)*. This indicates that testosterone plays a major role not only in
386 spermatogenesis but also in the functional maturation of sperm. In this study, metabolic
387 abnormalities induced by inhibition of androgen receptor function caused abnormal proliferation
388 of seminal vesicle epithelial cells in aged mice. In other words, the findings of the seminal vesicle
389 epithelial cell culture experiments and flutamide treatment may mimic the changes that occur
390 with aging. Oleic acid synthesis by testosterone-dependent metabolic pathways was regulated in

391 seminal vesicle epithelial cells. It could be assumed that a decrease in testosterone levels causes
392 abnormalities in the components of human semen. In particular, the results open up the
393 possibility of a translational study to detect low testosterone levels in men by testing for oleic
394 acid in semen.

395 Because seminal plasma contains components specific to certain male reproductive organs,
396 differences in protein composition may reflect pathological processes in these specific organs
397 *(59)*. However, although proteomic and metabolomic analyses of seminal plasma have been
398 performed *(31, 59)*, the functional changes in seminal plasma, especially the effects on *in vivo*
399 fertilization potential, are not fully understood. This is because there are many challenges to
400 measuring the direct relationship between sperm metabolism and movement patterns. It has been
401 suggested that the potential importance of the effect of oleic acid on improving fertility, yet it is
402 too early to conclude this in this study. If a direct causal relationship between fatty acid
403 composition and improved sperm motility is established, differences in the concentration of fatty
404 acids in the seminal plasma will become a predictive marker of the fertilizing ability of semen.
405 The interspecies differences between humans and mice should be interpreted with caution, and
406 the translational aspects to humans are speculative, but this study revealed a testosterone-
407 dependent mechanism of oleic acid production in seminal vesicle epithelium.

408 Overall, the results of the studies described herein strongly support the hypothesis that
409 testosterone-dependent glucose to oleic acid conversion processes are required for normal
410 seminal plasma functions in the seminal vesicle (Fig.9). This study advances our understanding
411 of the role of testosterone in glucose metabolism and fatty acid synthesis and lays the
412 groundwork for future research in reproductive biology and fertility.

413

414 **MATERIALS AND METHODS**

415 **Study design**

416 The objective of this study was to elucidate the mechanisms of seminal plasma synthesis.
417 Testosterone-dependent changes in the seminal plasma function were examined by comparative
418 analysis of adult mice and flutamide-treated mice. The bioassays of extracts from male accessory
419 glands by epididymal sperm motility analysis were used to examine the seminal plasma
420 components important for sperm function. We also isolated the mouse seminal vesicle epithelial

421 cultured cells, and investigated the synthesis mechanism of the seminal plasma components using
422 RNA-seq, FluxAnalyzer, and shRNA knockdown. Finally, we performed validation using the
423 human epithelial cells.
424
425 **Chemicals and Animals**
426 Unless otherwise noted, chemicals used in this study were purchased from Sigma-Aldrich (St.
427 Louis, MO, USA) or Nacalai tesque (Osaka, Japan). Equine chorionic gonadotropin (eCG) and
428 human chorionic gonadotropin (hCG) were purchased from Asuka Seiyaku (Tokyo, Japan). All
429 procedures during animal experiments were reviewed and approved by the Animal Care and Use
430 Committee of Hiroshima University (Hiroshima, Japan; C21-9-3) and conducted according to
431 regulations. Specific pathogen-free C57BL/6NCrl male mice or Crl: CD1 (ICR) female mice were
432 purchased from Jackson Laboratory Japan (Kanagawa, Japan) and housed in an environmentally
433 controlled room with a 12-hour light/dark cycle, a temperature of 23 ± 3°C, and free access to
434 laboratory food (MF; Oriental Yeast Co., Ltd., Tokyo, Japan) and tap water. 8- to 16-week-old
435 male or female mice were used for the experiments. Flutamide-treated mice were injected
436 subcutaneously for 7 days with 50 μg/g (body weight) of flutamide dissolved in corn oil. Vehicle-
437 treated mice received 100 μL of corn oil subcutaneously for 7 days. The aged males were 12 to
438 16 months old.
439
440 **Bioassay using pseudo-seminal plasma and epididymal sperm**
441 Prostate (mixed anterior, dorsal, lateral, and ventral) and seminal vesicles were collected from
442 adult C57BL/6NCrl mice. Seminal vesicle secretions were obtained by pressing the seminal
443 vesicles immediately after euthanasia. Prostatic extracts were obtained by homogenizing the
444 prostate immediately after euthanasia. Seminal vesicle secretions and prostate extracts collected
445 from one male mouse were dissolved in 500 μL and 200 μL of mHTF medium without BSA *(60)*,
446 respectively, then centrifuged at 2000 × g for 5 min at room temperature, and the supernatant was
447 collected, and protein levels were determined. The seminal vesicle secretions from flutamide-
448 treated mice were also collected similarly.
449 Cauda epididymis sperm recovered from male mouse were dispersed in 500 μL of mHTF
450 without BSA and centrifuged at 300 × g, 3 min to wash out epididymis-derived factors. The final

451 protein concentration of prostate and seminal vesicle secretion was adjusted to 10 mg/mL. An
452 aliquot (2 mL) of the pooled prostate or seminal vesicle extracts was conducted the viscosity
453 measurement data using Tuning Fork Vibro Viscometers (SV-1A, A&D Company, Tokyo, Japan).
454 The epididymis sperm was mixed with seminal vesicle secretion and/or prostate extract as shown
455 in Fig.1 and Supplementary Figure 1. The samples were incubated at 37°C for 60 min in a
456 humidified atmosphere of 5% CO2 in air. Sperm motility patterns were then examined using
457 computer-assisted sperm analysis (CASA; HT CASA-Ceros II, Hamilton Thorne, Beverly, MA,
458 USA), with software version 1.11.9. The following sperm motility parameters were analyzed:
459 percentage of motile sperm (denoted by a path velocity >40 μm/s and a VSL >20 μm/s),
460 percentage of motile sperm with progressive motility (denoted by a path velocity >40 μm/s and a
461 straightness ratio >60%). Straight-Line Velocity; VSL: The distance between the first and last
462 tracking points of the sperm trajectory divided by the elapsed time. Curvi-Linear Velocity; VCL:
463 The sum of the distances between the centers of brightness in each frame divided by the elapsed
464 time. Linearity; LIN: Measures the straightness of the path. LIN is derived from the ratio of
465 VSL/VCL multiplied by 100.
466
467 **Serum testosterone levels**
468 The serum was separated from the clot by centrifugation at 1,500 × g for 15 min. Testosterone
469 levels in the serum samples were determined by a rodent testosterone ELISA test kit (ERKR7016,
470 Endocrine Technologies, Inc., Newark, CA, USA) according to the manufacturer's manual.
471
472 **Mitochondrial activity**
473 Mitochondrial activity of sperm was measured using a MitoPT® JC-1 Assay Kit (911, Immuno
474 Chemistry Technologies, LLC, Bloomington, MN, USA) according to our previous study *(20)*.
475 Briefly, sperm were incubated with 200 μL of working solution containing 5,5',6,6'-tetrachloro-
476 1,1',3,3'-tetraethylbenzimidazolyl carbocyanine iodide (JC-1) dye at 37 °C for 30 min in the dark.
477 Using 10 μM of antimycin control (A8674; Sigma) under the same incubation conditions, we
478 confirmed that the JC-1 reaction is sensitive to changes in membrane potential. The sperm
479 suspension was centrifuged and washed twice with the base medium. After washing, the sperm
480 pellet was resuspended in the base medium and analyzed with an Attune® NxT Acoustic Focusing

481 Cytometer (Thermo Fisher Scientific Inc., Waltham, MA, USA) using a 488 nm laser and a filter
482 with a bandwidth of 574/26 nm. The intensity of the average value was analyzed as the mean
483 fluorescence intensity (MFI) of JC-1 orange aggregates. A total of 100,000 sperm events were
484 analyzed. The sperm population is shown in Supplementary Figure 6.
485
486 ***In vitro* fertilization (IVF)**
487 3 weeks old CD1 female mice were injected intraperitoneally with 4IU eCG to stimulate
488 follicle development and 5 IU hCG at 48 hours later. COCs collected from the oviductal
489 ampulla 16 h after hCG injection were placed into 100 μL of human tubal fluid (HTF) medium.
490 Sperm were collected from the cauda epididymis of 15 weeks or older C57BL/6N male mice in
491 100 μL of HTF medium. After 60 min of incubation with or without treatments (Ctrl, Flu or
492 HTF), the sperm were added into HTF medium at a final concentration of
493 2×10^5 spermatozoa/mL, and coincubated with the COCs. After 6h incubation, oocytes were
494 washed three times thoroughly and cultured in 250 μL of KSOM medium (MR 106-D; Sigma).
495 The cleavage rate was determined on Day 1 (Day 0=day of IVF), and the appearance of
496 blastocysts was recorded on Day 5.
497
498 **Immunohistochemistry and immunofluorescence**
499 Seminal vesicles were fixed overnight in 4% (w/v) paraformaldehyde/PBS, dehydrated in 70%
500 (v/v) ethanol, and embedded in paraffin. Paraffin-embedded fixed sections (4 μm) were
501 deparaffinized and hydrated with xylene and ethanol, respectively. Some slides were stained with
502 hematoxylin and eosin (HE). For antigen retrieval, sections were placed in citrate buffer (pH 6.0),
503 microwaved until boiling and allowed to stand at the temperature of pre-boil (95°C) for 15
504 minutes. Sections were incubated with 3% (v/v) hydrogen peroxide in methanol to block
505 endogenous peroxidase and then incubated with Normal Goat Serum Blocking Solution for rabbit
506 antibody (S-1000, Vector Laboratories, Newark, CA, USA) to block nonspecific sites. The
507 sections were then incubated overnight with primary rabbit antibodies: anti-AR antibody (1:100;
508 ab133273; Abcam, Cambridge, UK), anti-Ki67 antibody (1:1000; ab15580; Abcam) or anti-
509 ACLY antibody (1:200; ab40793; Abcam). Positive signals were visualized by DAB (3,3′-
510 Diaminobenzidine, 040-27001, Fujifilm Wako, Osaka, Japan) using the VECTASTAINE

511 LifeABC kit (PK-6101, Vector Laboratories) according to the manufacturer's protocol. Apoptotic
512 cells (including fragmented DNA) were detected using the In Situ Cell Death Detection Kit POD
513 (11684817910, Roche Ltd., Basel, Switzerland). To avoid false-positive or false-negative results,
514 DNAse-treated sections were used as positive controls, and TdT-untreated sections were used as
515 negative controls for apoptosis.
516 Nuclei were visualized with hematoxylin (Sakura Finetek, Tokyo, Japan). Ki-67 and apoptotic
517 positive cells were quantified using ImageJ software (National Institutes of Health; Bethesda, MD,
518 USA), with software version 2.1.0/1.53u. Randomly selected sections were stained, and images
519 were obtained from randomly selected fields in each section. The positive percentage is defined
520 as the percentage of positively stained cells in the total number of epithelial cells evaluated. Only
521 positive staining was considered, regardless of staining intensity. For immunofluorescence, after
522 blocking nonspecific sites, the sections were incubated with a primary antibody: anti-GLUT4
523 antibody (1:200; ab33780; Abcam). After washing with 0.3% (v/v) Triton X-100 in PBS (-), Cy3-
524 labeled goat anti-rabbit IgG (1:200, C-2306, Sigma) and DAPI (VECTESHIELD Mounting
525 Medium with DAPI, H-1200, Vector Laboratories) were used to visualize the antigen and nuclei.
526 Digital images were taken using an APX100 Digital Imaging System and CellSens imaging
527 software (EVIDENT, Tokyo, Japan), with software version 4.1.1.
528
529 **Isolation and culture of seminal vesicle epithelial cells**
530 Seminal vesicles were removed from euthanized mice, cut open vertically to expose the seminal
531 vesicle cavity, and incubated with Hanks' balanced salt solution (HBSS; $CaCl_2 \cdot 2H_2O$ 0.185 g/L,
532 $MgSO_4$ 0.098 g/L, KCl 0.400 g/L, KH_2PO_4 0.060 g/L, NaHCO3 0.350 g/L, NaCl 8.000 g/L,
533 Na_2HPO_4 0.048 g/L, D-Glucose 1.0 g/L, dissolved in ultrapure water). Tissues were digested with
534 10 mL of HBSS containing 25 mg/mL pancreatin and 0.25% (v/v) trypsin EDTA for 1 hour at
535 4°C, 45 minutes at room temperature, and 15 minutes at 37°C, and epithelial cells were obtained.
536 These were passed through a 70 μm nylon filter (352350, Corning Inc., Corning, NY, USA) and
537 seeded into collagen-coated 12-well plates (4815-010, IWAKI, Shizuoka, Japan). Cells were
538 cultured in DMEM/F-12, 10% fetal bovine serum (FBS; 10438-018, Thermo Fisher Scientific
539 Inc.), 100 U/mL penicillin, 100 μg/mL streptomycin. The culture condition was 37°C, 5% CO_2,
540 95% air, and humidity.

541 Human seminal vesicle epithelial cells (4460, ScienCell Research Laboratories, Carlsbad, CA,
542 USA) were purchased, seeded in 2 μg/cm^2 poly-L-lysine-coated plates, and cultured in epithelial
543 cell medium (4101, ScienCell Research Laboratories). The cells were seeded at 10000 cells/cm^2
544 on collagen-coated plates the day before 100 ng/mL testosterone treatment. Testosterone was
545 dissolved in ethanol, and the final concentration of ethanol was adjusted to 0.1% (v/v) when used
546 for cultured cells. The culture medium was replaced every 48 hours.
547
548 **Cell proliferation curve**
549 The seminal vesicle epithelial cells were seeded at 10000 cells/cm^2 and then were cultured in
550 various concentrations of testosterone. The cells were washed with HBSS (without $CaCl_2$-
551 $2H_2O/MgSO_4$) at the time of cell counting and collected using 0.25% (v/v) trypsin. The recovered
552 cells were suspended in DMEM/F-12 medium, and cell numbers were determined using an
553 Automated Cell Counter TC20TM (BIO-RAD Laboratories, Hercules, CA, USA) to calculate the
554 number of cells contained per well (4 cm^2).
555
556 **Cell cycle analysis**
557 The recovered cells as described above were fixed in 2-5 ml of cold (4°C) 70% methanol for
558 at least 30 minutes on ice. After centrifugation at 500g for 5 minutes at 4°C to obtain pellets, the
559 cell pellet was suspended in 50 μM propidium iodide and 20 × diluted RNase (19101, QIAGEN
560 Inc., Venlo, Netherlands) and then were incubated at 37°C for 30 minutes. After twice washing
561 with 1 ml of PBS at 300 g for 3 min at 4°C, the cells were analyzed by flow cytometry. The cell
562 population is shown in Supplementary Figure 8. A total of 20,000 events were analyzed.
563
564 **RNA-sequencing**
565 Total RNA was extracted from cells using the RNeasy Mini Kit (74106, QIAGEN). Three
566 independent samples were assayed to evaluate the reproducibility of the experimental procedures.
567 The quality of total RNA (1 μg) submitted for sequencing was checked using a Bioanalyzer
568 (Agilent Technologies Inc., Santa Clara, CA, USA), and all RNA integrity numbers were >7.0.
569 The libraries for RNA sequencing were sequenced with 2 × 150-bp paired-end reads on a
570 NovaSeq6000 (Illumina Inc., San Diego, CA, USA). The obtained sequencing data were analyzed

571 using RaNA-seq *(61)*, an open bioinformatics tool for rapid RNA-seq data analysis. FASTQ files
572 were preprocessed in the pipeline using the Fastp tool, and expression was quantified using
573 Salmon. DEseq2 was used to identify differentially expressed genes (DEGs) with adjusted p-
574 values less than 0.05 between the testosterone-treated groups in transcripts per million (TPM)
575 between control and testosterone-treated cells. The pathways were identified from the KEGG
576 database on RaNA-seq.
577
578 **Extracellular flux analysis**
579 Oxygen consumption rate (OCR) and ECAR were measured using an extracellular flux
580 analyzer (XF HS Mini; Agilent Technologies). Eight-well plates for the XF HS Mini were coated
581 with fibronectin (5 μg/mL, F1141, Sigma-Aldrich) dissolved in phosphate-buffered saline (PBS),
582 incubated overnight, and then washed with Roswell Park Memorial Laboratory medium for XF
583 (Roswell Park Memorial Institute medium; RPMI, 103576-100, Agilent Technologies; containing
584 1% FBS) for XF before analysis. Mouse seminal vesicle epithelial cells or human seminal vesicle
585 epithelial cells treated with 100 ng/mL testosterone for 7 days were suspended in RPMI medium
586 at a concentration of 10,000 cells/180 μL, or mouse seminal vesicle epithelial cells infected with
587 shRNA were suspended at a concentration of 2000 cells/180 μL in each well. After centrifugation
588 at 300 × g for 3 minutes, the plates were placed in an incubator at 37°C and 100% air and used
589 for analysis within 1 hour.
590 For glucose metabolism assessment, cells were sequentially treated as indicated with D-
591 Glucose (10 mM; 103577-100, Agilent Technologies), Oligomycin (1 μM; O4876, Sigma-
592 Aldrich), and 2-Deoxy-Glucose (50 mM; D8375, Sigma-Aldrich).
593 For mitochondrial respiration measurement, cells were sequentially treated as indicated with
594 Oligomycin (1 μM), carbonyl cyanide 4-(trifluoromethoxy) phenylhydrazone (FCCP; 5 μM,
595 SML2959, Sigma-Aldrich), and Rotenone (1 μM; R8875, Sigma-Aldrich)/Antimycin A (1 μM;
596 A8674, Sigma-Aldrich). Cellular metabolism readouts, such as glycolysis, glycolytic reserve,
597 basal OCR, Maximum respiration, ATP Production, Spare respiratory capacity, were determined
598 using the Agilent Seahorse Wave software with software version 3.0.0.41. However, to avoid
599 many ambiguities and problems with interpretation, “glycolysis” is written as “Glucose-induced

600 ECAR", "glycolytic reserve" as "Oligomycin-sensitive ECAR", "maximum respiration" as
601 "FCCP uncoupled respiration", and "ATP production" as "Oligomycin-sensitive respiration".
602
603 **Measurement of pyruvate and lactic acid**
604 For measurements, mouse or human seminal vesicle epithelial cells were treated with 100
605 ng/ml testosterone for 6 days. The culture supernatant was collected after 24 hr of additional
606 culture. Pyruvate consumption was measured using the Pyruvate Assay kit (MET-5029, Cell
607 Biolabs, Inc., San Diego, CA, USA). The fluorescence intensity was measured using a microplate
608 reader (ex. 570 nm/em. 615 nm). Lactate released into the medium was measured using the
609 Lactate Assay kit (L256, DOJINDO LABOLATORIES Co., Ltd., Kumamoto, Japan). The
610 absorbance was measured using a microplate reader (wave length=450nm).
611
612 **qPCR**
613 The cDNA was synthesized from 40 ng of total RNA using oligo$(dT)_{15}$ primers (3805, Takara
614 Bio Inc., Shiga, Japan) and an Avian myeloblastosis virus (AMV) reverse transcriptase from
615 Promega (M5101, Madison, WI, USA). The cDNA and primers were added to Power SYBR
616 Green PCR Master Mix (4367659, Applied Biosystems, Foster City, CA, USA) in a total reaction
617 volume of 15 µl. Conditions were set to the following parameters: 10 min at 95°C, 15 sec at 95°C,
618 and 1 min at 60°C. Cycles were repeated 45 times. Specific primer pairs were selected and
619 analyzed, as shown in Table S1. Expression was first normalized to housekeeping gene *Rpl19*,
620 and fold change was calculated relative to the mean of the control samples.
621
622 **Glucose uptake test of seminal vesicle epithelial cells and lipid determination of culture**
623 **supernatants**
624 Mouse or human seminal vesicle epithelial cells treated with or without 100 ng/mL testosterone
625 for 6 days were used for this experiment. Cells were treated with or without the GLUT4 inhibitor
626 indinavir (100 nM) and 100 ng/mL testosterone for an additional 24 hours. Collected 15,000 cells
627 were subjected to Glucose Uptake Assay Kit-Green (UP02; DOJINDO), and fluorescence
628 intensity was measured using a microplate reader (ex. 485 nm/em. 535 nm).

629 Total lipid content in cultured medium was quantified using a lipid quantification kit (STA-617
630 Fluorometric, Cell Biolabs, Inc.) according to the manufacturer's protocol. The fluorescence
631 intensity was measured using a microplate reader (ex. 485 nm/em. 535 nm).
632
633 **Gas chromatography-mass spectrometry analysis**
634 Fatty acid measurements in culture supernatant and seminal vesicle secretions were done
635 according to our previous work *(21)*. Fatty acids in the samples were extracted and methylated
636 using a fatty acid methylation kit (06482-04, Nacalai Tesque) and then purified using a fatty acid
637 methyl ester purification kit (06483-94, Nacalai Tesque). The methylated sample (3.0 mL) was
638 dried and dissolved in 50 μL of elution solution. Samples were subjected to GC-MS.
639 Fatty acids were determined on an Agilent 7890A GC system coupled with a JMS-T 100 GCv
640 mass detector at the Natural Science Research Center, Hiroshima University (N-BARD). Sample
641 (1.0 μL aliquot) was injected to SP®-2560 capillary GC column (100 m × 0.25 mm i.d. × 0.2 μm
642 film thickness; 24056, Sigma-Aldrich). For measurements, helium was used as the carrier gas at
643 a constant flow rate of 2.0 mL/min. The GC oven temperature was gradually increased from
644 100°C to 300°C at a rate of 10°C/min and held at 300°C for 20 minutes. Ionization was performed
645 using electron ionization with an electron energy of 70 eV. Mass spectra were obtained in scan
646 mode (mass scan range 29-800 m/z). NIST MS Search v.2.0 was used to detect and identify of
647 fatty acids.
648
649 **Sperm motility parameters with the lipid Mixture**
650 Sperm recovered from the cauda epididymis of male mice were dispersed in 500 μL of mHTF
651 without BSA and centrifuged at 300 × g for 3 minutes to wash out epididymis-derived factors.
652 The sperm pellets were resuspended in HTF medium with or without a lipid mixture (LM) that
653 included 2 μg/mL arachidonic acid, 10 μg/mL linoleic acid, 10 μg/mL linolenic acid, 10 μg/mL
654 myristic acid, 10 μg/mL oleic acid, 10 μg/mL palmitic acid, and 10 μg/mL stearic acid (L0288,
655 Sigma-Aldrich). The sperm were then incubated for 60 minutes at 37°C under a humidified
656 atmosphere of 5% CO2. Sperm motility patterns were subsequently examined using CASA.
657
658 **ACLY knock down experiment using shRNA**

659 The U6 shRNA lentiviral vector of the *Acly* gene (mAcly[shRNA#1]; a virus packaging service,
660 VectorBuilder, Chicago, IL, USA) was used for knockdown experiments. The ACLY sequence
661 targeted by the shRNA vector used in this study was 5′-GCAGCAAAGATGTTCAGTAAA-3′.
662 Lentivirally transduced cells were prepared according to manufacture protocol. Immediately after
663 isolation, the mouse seminal vesicle epithelial cells were cultured overnight in a medium
664 containing 5 μg/mL polybrene (VectorBuilder) and lentiviral particles expressing an shRNA
665 targeting ACLY or a scramble (Multiplicity of Infection of 10). After an additional overnight
666 incubation in a fresh culture medium, the cells were incubated for 5 days in a medium containing
667 1 μg/ml puromycin (19752-64, Nacalai tesque). 100 ng/mL of testosterone was added to all
668 procedures for the testosterone-treated group. Infection efficiency, calculated based on the
669 number of GFP-positive cells using an APX100 Digital Imaging System, ranged between 70%
670 and 90%.
671 For sperm motility analysis, sperm were collected and washed with mHTF from the culture
672 supernatant and cauda epididymis. The samples were incubated at 37°C for 60 minutes in a
673 humidified atmosphere of 5% CO2 in air. The sperm motility pattern was then examined using
674 CASA.
675
676 **Western blot analysis**
677 Protein samples of mouse seminal vesicle epithelial cells, seminal vesicle tissue, and sperm
678 were prepared by homogenization in cell lysis buffer (04719964001, cOmplete™ Lysis-M
679 EDTA-free, Roche) and diluted with an equal volume of sample buffer solution containing 2-ME
680 (2 ×) for SDS-PAGE (30566-22, Nacalai tesque). The extracts (10 μg protein) were separated by
681 SDS-polyacrylamide gel (10%) electrophoresis and transferred to polyvinylidene fluoride
682 membranes (10600069, Cytiva, Tokyo, Japan). The membranes were then treated with Tris-
683 buffered saline and Tween 20 (TBST, 20 mM Tris, pH 7.5, 150 mM NaCl, 0.1% Tween 20)
684 containing 5% (w/v) Non-Fat Dry milk (MORINAGA MILK INDUSTRY Co., Ltd., Tokyo,
685 Japan) for the nonspecific reaction was blocked. The membranes were incubated overnight at 4°C
686 with primary antibodies: anti-GLUT4 antibody (1:100; ab33780; Abcam), anti-ACLY antibody
687 (1:10,000; ab40793; Abcam) or anti-α/β-Tubulin antibody (1:1,000; 2148S; Cell Signaling). The
688 next day, membranes were washed with TBST and incubated with HRP-labeled antibody specific

for rabbit IgG (1:4000; 7074S; Cell Signaling). The bands were visualized by using Enhanced Chemiluminescence detection systems (RPN2232, Cytiva) and ChemiDoc™ MP Imaging System (BIO-RAD Laboratories). The bands were analyzed by using the software ImageJ. Densitometry analysis was performed using the ImageJ Gel Analysis tool, and the background of the gel was also removed individually for each band. The full-length blotting images are shown in Supplementary Figure 7.

Statistical analysis

Quantitative data were presented as means ± SEM. The Bartlett's test was used to confirm whether the variances were equal for each group in experiments consisting of three or more groups. All statistical details of the experiments are given in the figure legends. R [(version 4.3.1 (2023-06-16)] was used for statistical analysis. Data were considered statistically significant at $p < 0.05$.

Data availability

Nucleotide sequence data reported are available in the DDBJ Sequenced Read Archive under the accession numbers DRA017090. Additional information needed to reanalyze the data reported in this paper is available from the principal contact upon request.

List of Supplementary Materials

Supplemental Figures 1 to 8

Table S1

Acknowledgments:

The authors would like to thank JoAnne S. Richards for carefully proofreading the manuscript and useful comments.

Funding:

This work was supported in part by JSPS KAKENHI Grant Number 23K14069 to TU and 23H00361 to MS.

Author contributions:

Conceptualization: TY, TU, MS

Methodology: TY, ZX, NT, MA, TU

Investigation: TY, ZX, NT, MA, TU

Visualization: TY, MS

Funding acquisition: TU, MS

Supervision: MS

Writing – original draft: TY

Writing – review & editing: TY, TU, MS

Competing interests:

MS holds stocks in and receives a salary from Hiroshima Cryopreservation Service Co. as a director. In addition, MS has received royalties and grants from Hiroshima Cryopreservation Service Co. M.S. has received consulting fees from Rohto Pharmaceutical Co., Ltd.. TU holds stocks in and receives a salary from Lullabio Inc. as a director and has received honoraria from Rohto Pharmaceutical Co., Ltd. The other authors declare they have no competing interests.

References

1. World Health Organization., Infertility prevalence estimates: 1990–2021. *Global report* , 1–98 (2023).

2. S. A. Kidd, B. Eskenazi, A. J. Wyrobek, Effects of male age on semen quality and fertility: a review of the literature. *Fertil Steril* **75**, 237–248 (2001).

3. A. Mumcu, A. Karaer, B. Dogan, G. Tuncay, Metabolomics analysis of seminal plasma in patients with idiopathic Oligoasthenoteratozoospermia using high-resolution NMR spectroscopy. *Andrology* **8**, 450–456 (2020).

4. Y. Xu, H. Lu, Y. Wang, Z. Zhang, Q. Wu, Comprehensive metabolic profiles of seminal plasma with different forms of male infertility and their correlation with sperm parameters. *J Pharm Biomed Anal* **177**, 112888 (2020)

5. S. Elbashir, Y. Magdi, A. Rashed, R. Henkel, A. Agarwal, Epididymal contribution to male

749 infertility: An overlooked problem. *Andrologia* **53**, e13721 (2021).
750 6. M. J. Cosentino, A. T. K. Cockett, Review Article: Structure and Function of the Epididymis
751 Transport of Spermatozoa. *Urol Res* **14**, 229–240 (1986).
752 7. B. Howarth, Fertilizing ability of cock spermatozoa from the testis epididymis and vas deferens
753 following intramagnal insemination. *Biol Reprod* **28**, 586–590 (1983).
754 8. R. Yanagimachi, The movement of golden hamster spermatozoa before and after capacitation.
755 *J Reprod Fertil* **23**, 193–196 (1970).
756 9. R. Yanagimachi, Mammalian Fertilization. E. Knobil, J.D. Neill (Eds.), *The physiology of*
757 *reproduction*, Raven Press, 189–317 (1994).
758 10. P. Gaddum-Rosse, Some observations on sperm transport through the uterotubal junction of
759 the rat. *Am J Anat* **160**, 333–341 (1981).
760 11. R. Shalgi, T. T. Smith, R. Yanagimachi, A Quantitative Comparison of the Passage of
761 Capacitated and Uncapacitated Hamster Spermatozoa through the Uterotubal Junction. *Biol*
762 *Reprod* **46**, 419–424 (1992).
763 12. H. Li, P. Hung, S. S. Suarez, Ejaculated Mouse Sperm Enter Cumulus-Oocyte Complexes
764 More Efficiently In Vitro than Epididymal Sperm. *PLoS One* **10**, e0127753 (2015)
765 13. T. Noda, M. Ikawa, Physiological function of seminal vesicle secretions on male fecundity.
766 *Reprod Med Biol* **18**, 241–246 (2019).
767 14. P. Verze, T. Cai, S. Lorenzetti, The role of the prostate in male fertility, health and disease. *Nat*
768 *Rev Urol* **13**, 379–386 (2016).
769 15. E. Balandya, W. Wieland-Alter, K. Sanders, T. Lahey, Human Seminal Plasma Fosters CD4+
770 Regulatory T-cell Phenotype and Transforming Growth Factor-β1 Expression. *American Journal*
771 *of Reproductive Immunology* **68**, 322–330 (2012).
772 16. T. Shima, K. Inada, A. Nakashima, A. Ushijima, M. Ito, O. Yoshino, S. Saito, Paternal antigen-
773 specific proliferating regulatory T cells are increased in uterine-draining lymph nodes just before
774 implantation and in pregnant uterus just after implantation by seminal plasma-priming in
775 allogeneic mouse pregnancy. *J Reprod Immunol* **108**, 72–82 (2015).
776 17. N. Kawano, N. Araki, K. Yoshida, T. Hibino, N. Ohnami, M. Makino, S. Kanai, H. Hasuwa,
777 M. Yoshida, K. Miyado, A. Umezawa, Seminal vesicle protein SVS2 is required for sperm
778 survival in the uterus. *Proc Natl Acad Sci U S A* **111**, 4145–4150 (2014).

18. R. R. Rosecrans, R. S. Jeyendran, M. Perez-Pelaez, W. P. Kennedy, Comparison of Biochemical Parameters of Human Blood Serum and Seminal Plasma. *Andrologia* **19**, 625–628 (1987).

19. T. Umehara, T. Kawai, M. Goto, J. A. S. Richards, M. Shimada, Creatine enhances the duration of sperm capacitation: a novel factor for improving in vitro fertilization with small numbers of sperm. *Human Reproduction* **33**, 1117–1129 (2018).

20. Z. Zhu, T. Kawai, T. Umehara, S. A. M. Hoque, W. Zeng, M. Shimada, Negative effects of ROS generated during linear sperm motility on gene expression and ATP generation in boar sperm mitochondria. *Free Radic Biol Med* **141**, 159–171 (2019).

21. M. M. Islam, T. Umehara, N. Tsujita, M. Shimada, Saturated fatty acids accelerate linear motility through mitochondrial ATP production in bull sperm. *Reprod Med Biol* **20**, 289–298 (2021).

22. T. Noda, Y. Fujihara, T. Matsumura, S. Oura, S. Kobayashi, M. Ikawa, Seminal vesicle secretory protein 7, PATE4, is not required for sperm function but for copulatory plug formation to ensure fecundity. *Biol Reprod* **100**, 1035–1045 (2019).

23. K. Queen, C. B. Dhabuwala, C. G. Pierrepoint, The effect of the removal of the various accessory sex glands on the fertility of male rats. *J Reprod Fertil* **62**, 423–426 (1981).

24. Mann T, Studies on the metabolism of semen; fructose as a normal constituent of seminal plasma; site of formation and function of fructose in semen. *Biochem J* **40**, 481–491 (1946).

25. Humphrey GF, Mann T, Studies on the metabolism of semen; citric acid in semen. *Biochem J* **44**, 97–105 (1949).

26. C. Chang, S. O. Lee, R. S. Wang, S. Yeh, T. M. Chang, Androgen receptor (AR) physiological roles in male and female reproductive systems: lessons learned from AR-knockout mice lacking AR in selective cells. *Biol Reprod* **89**, 1–16 (2013).

27. C. Fix, C. Jordan, P. Cano, W. H. Walker, Testosterone activates mitogen-activated protein kinase and the cAMP response element binding protein transcription factor in Sertoli cells. *Proc Natl Acad Sci U S A* **101**, 10919–10924 (2004).

28. K. Nagaosa, A. Kishimoto, R. Kizu, A. Nakagawa, A. Shiratsuchi, Y. Nakanishi, Perturbation of spermatogenesis by androgen antagonists directly injected into seminiferous tubules of live mice. *Reproduction* **133**, 21–27 (2007).

29. L. B. Smith, W. H. Walker, The regulation of spermatogenesis by androgens. *Semin Cell Dev Biol* **30**, 2–13 (2014).

30. P. S. Cooke, W. H. Walker, Male fertility in mice requires classical and nonclassical androgen signaling. *Cell Rep* **36**, 109557 (2021).

31. S. P. Smyth, B. Nixon, A. L. Anderson, H. C. Murray, J. H. Martin, L. A. MacDougall, S. A. Robertson, D. A. Skerrett-Byrne, J. E. Schjenken, Elucidation of the protein composition of mouse seminal vesicle fluid. *Proteomics* **22**, e2100227 (2022).

32. H. Murata, P. W. Hruz, M. Mueckler, Indinavir inhibits the glucose transporter isoform Glut4 at physiologic concentrations. *AIDS* **16**, 859–863 (2002).

33. C. Wilson, A. Contreras-Ferrat, N. Venegas, C. Osorio-Fuentealba, M. Pávez, K. Montoya, J. Durán, R. Maass, S. Lavandero, M. Estrada, Testosterone increases GLUT4-dependent glucose uptake in cardiomyocytes. *J Cell Physiol* **228**, 2399–2407 (2013).

34. G. F. Gonzales, Function of seminal vesicles and their role on male fertility. *Asian J Androl* **3**, 251–258 (2001).

35. A. Lenzi, M. Picardo, L. Gandini, F. Dondero, Lipids of the sperm plasma membrane: from polyunsaturated fatty acids considered as markers of sperm function to possible scavenger therapy. *Hum Reprod Update* **2**, 246–256 (1996).

36. M. T. Haren, A. M. Siddiqui, H. J. Armbrecht, R. T. Kevorkian, M. J. Kim, M. J. Haas, A. Mazza, V. B. Kumar, M. Green, W. A. Banks, J. E. Morley, Testosterone modulates gene expression pathways regulating nutrient accumulation, glucose metabolism and protein turnover in mouse skeletal muscle. *Int J Androl* **34**, 55–68 (2011).

37. L. C. Costello, R. B. Franklin, Testosterone and prolactin regulation of metabolic genes and citrate metabolism of prostate epithelial cells. *Horm Metab Res* **34**, 417–424 (2002).

38. K. Gonthier, R. T. K. Poluri, É. Audet-Walsh, Functional genomic studies reveal the androgen receptor as a master regulator of cellular energy metabolism in prostate cancer. *J Steroid Biochem Mol Biol* **191**, 105367 (2019).

39. M. F. Troncoso, M. Pavez, C. Wilson, D. Lagos, J. Duran, S. Ramos, G. Barrientos, P. Silva, P. Llanos, C. Basualto-Alarcón, B. D. Westenbrink, S. Lavandero, M. Estrada, Testosterone activates glucose metabolism through AMPK and androgen signaling in cardiomyocyte hypertrophy. *Biol Res* **54**, 1–16 (2021).

839 40. Chen X, Li X, Huang HY, Li X, Lin JF, Effects of testosterone on insulin receptor substrate-
840 1 and glucose transporter 4 expression in cells sensitive to insulin. *Zhonghua Yi Xue Za Zhi* **86**,
841 1474–1477 (2006).
842 41. K. Sato, M. Iemitsu, K. Aizawa, R. Ajisaka, Testosterone and DHEA activate the glucose
843 metabolism-related signaling pathway in skeletal muscle. *Am J Physiol Endocrinol Metab* **294**,
844 E961–E968 (2008).
845 42. P. K. Arnold, B. T. Jackson, K. I. Paras, J. S. Brunner, M. L. Hart, O. J. Newsom, S. P.
846 Alibeckoff, J. Endress, E. Drill, L. B. Sullivan, L. W. S. Finley, A non-canonical tricarboxylic acid
847 cycle underlies cellular identity. *Nature* **603**, 477–481 (2022).
848 43. A. Luengo, Z. Li, D. Y. Gui, L. B. Sullivan, M. Zagorulya, B. T. Do, R. Ferreira, A. Naamati,
849 A. Ali, C. A. Lewis, C. J. Thomas, S. Spranger, N. J. Matheson, M. G. Vander Heiden, Increased
850 demand for NAD+ relative to ATP drives aerobic glycolysis. *Mol Cell* **81**, 691–707 (2021).
851 44. B. B. Yeap, Testosterone and cardiovascular disease risk. *Curr Opin Endocrinol Diabetes*
852 *Obes* **22**, 193–202 (2015).
853 45. J. D. Marsh, M. H. Lehmann, R. H. Ritchie, J. K. Gwathmey, G. E. Green, R. J. Schiebinger,
854 Androgen receptors mediate hypertrophy in cardiac myocytes. *Circulation* **98**, 256–261 (1998).
855 46. G. F. Grabner, H. Xie, M. Schweiger, R. Zechner, Lipolysis: cellular mechanisms for lipid
856 mobilization from fat stores. *Nat Metab* **3**, 1445–1465 (2021).
857 47. B. Mittendorfer, Origins of metabolic complications in obesity: adipose tissue and free fatty
858 acid trafficking. *Curr Opin Clin Nutr Metab Care* **14**, 535–541 (2011).
859 48. H. Wackerhage, I. J. Vechetti, P. Baumert, S. Gehlert, L. Becker, R. T. Jaspers, M. H. de
860 Angelis, Does a Hypertrophying Muscle Fibre Reprogramme its Metabolism Similar to a Cancer
861 Cell? *Sports Med* **52**, 2569–2578 (2022).
862 49. R. J. De Berardinis, N. S. Chandel, Fundamentals of cancer metabolism. *Sci Adv* **2**, e1600200
863 (2016).
864 50. G. L. Semenza, Hypoxia-inducible factors in physiology and medicine. *Cell* **148**, 399–408
865 (2012).
866 51. B. Morant-Ferrando, D. Jimenez-Blasco, P. Alonso-Batan, J. Agulla, R. Lapresa, D. Garcia-
867 Rodriguez, S. Yunta-Sanchez, I. Lopez-Fabuel, E. Fernandez, P. Carmeliet, A. Almeida, M.
868 Garcia-Macia, J. P. Bolaños, Fatty acid oxidation organizes mitochondrial supercomplexes to

869 sustain astrocytic ROS and cognition. *Nat Metab* **5**, 1290–1302 (2023).
870 52. M. Duta-Mare, V. Sachdev, C. Leopold, D. Kolb, N. Vujic, M. Korbelius, D. C. Hofer, W. Xia,
871 K. Huber, M. Auer, B. Gottschalk, C. Magnes, W. F. Graier, A. Prokesch, B. Radovic, J. G.
872 Bogner-Strauss, D. Kratky, Lysosomal acid lipase regulates fatty acid channeling in brown
873 adipose tissue to maintain thermogenesis. *Biochim Biophys Acta Mol Cell Biol Lipids* **1863**, 467–
874 478 (2018).
875 53. S. C. C. Huang, B. Everts, Y. Ivanova, D. O'Sullivan, M. Nascimento, A. M. Smith, W. Beatty,
876 L. Love-Gregory, W. Y. Lam, C. M. O'Neill, C. Yan, H. Du, N. A. Abumrad, J. F. Urban, M. N.
877 Artyomov, E. L. Pearce, E. J. Pearce, Cell-intrinsic lysosomal lipolysis is essential for alternative
878 activation of macrophages. *Nat Immunol* **15**, 846–855 (2014).
879 54. K. H. Tsui, T. H. Feng, Y. F. Lin, P. L. Chang, H. H. Juang, p53 downregulates the gene
880 expression of mitochondrial aconitase in human prostate carcinoma cells. *Prostate* **71**, 62–70
881 (2011).
882 55. S. Almeida, L. Rato, M. Sousa, M. G. Alves, P. F. Oliveira, Fertility and Sperm Quality in the
883 Aging Male. *Curr Pharm Des* **23**, 4429–4437 (2017).
884 56. T. Murata, Y. Ishitsuka, K. Karouji, H. Kaneda, H. Toki, Y. Nakai, S. Makino, R. Fukumura,
885 H. Kotaki, S. Wakana, T. Noda, Y. Gondo, β-cateninC429S mice exhibit sterility consequent to
886 spatiotemporally sustained Wnt signalling in the internal genitalia. *Sci Rep* **4**, 6959 1–7 (2014).
887 57. B. A. Stone, A. Alex, L. B. Werlin, R. P. Marrs, Age thresholds for changes in semen
888 parameters in men. *Fertil Steril* **100**, 952–958 (2013).
889 58. J. L. Frattarelli, K. A. Miller, B. T. Miller, K. Elkind-Hirsch, R. T. Scott, Male age negatively
890 impacts embryo development and reproductive outcome in donor oocyte assisted reproductive
891 technology cycles. *Fertil Steril* **90**, 97–103 (2008).
892 59. A. P. Drabovich, P. Saraon, K. Jarvi, E. P. Diamandis, Seminal plasma as a diagnostic fluid
893 for male reproductive system disorders. *Nat Rev Urol* **11**, 278–288 (2014).
894 60. T. Umehara, N. Tsujita, Z. Zhu, M. Ikedo, M. Shimada, A simple sperm-sexing method that
895 activates TLR7/8 on X sperm for the efficient production of sexed mouse or cattle embryos. *Nat*
896 *Protoc* **15**, 2645–2667 (2020).
897 61. C. Prieto, D. Barrios, RaNA-Seq: Interactive RNA-Seq analysis from FASTQ files to
898 functional analysis. *Bioinformatics* **36**, 1955–1956 (2019).

908 **Figures and Figure legends**

909 **Fig.1**

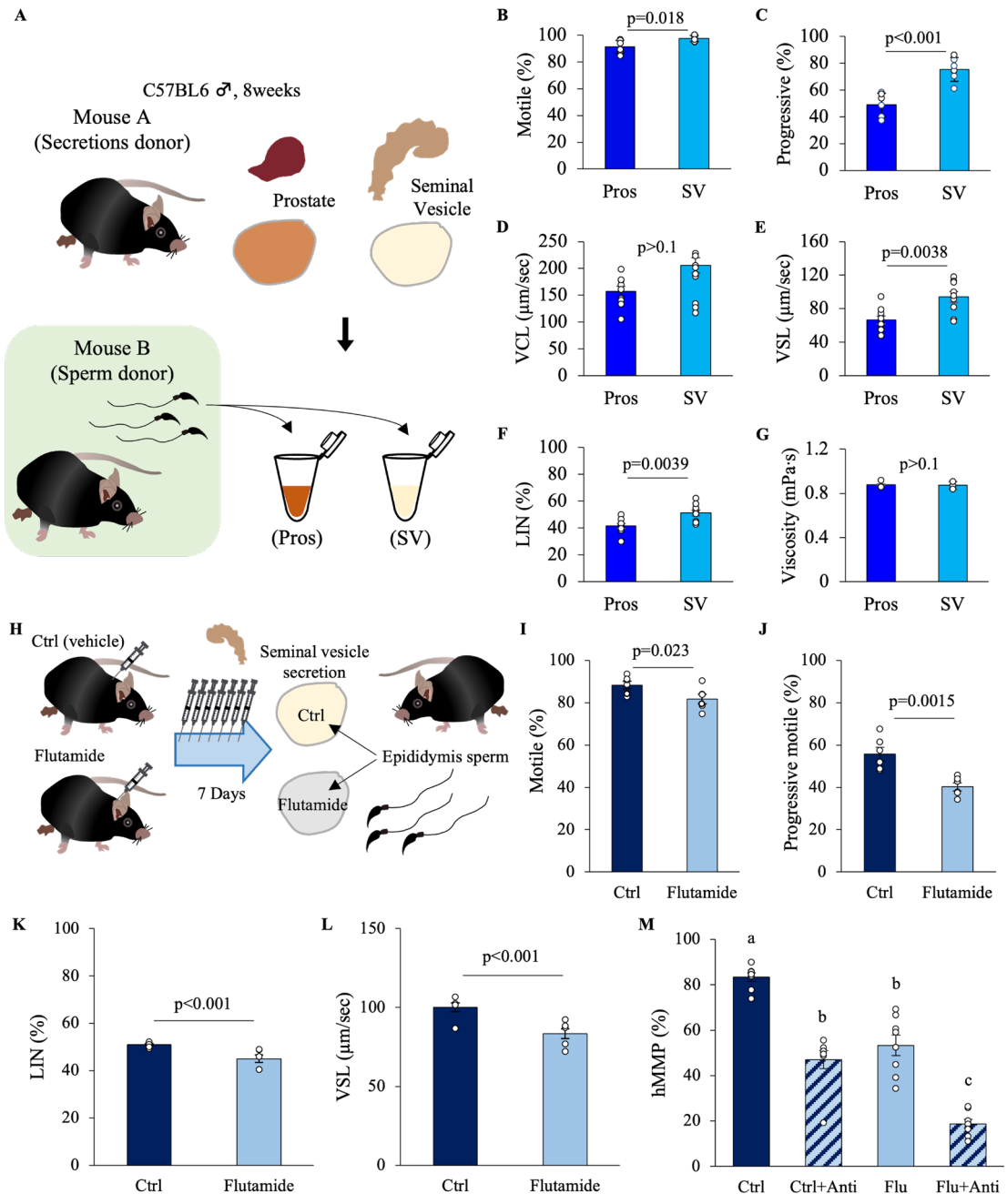

910

911 **Figure 1. Effects of seminal vesicle fluid and prostate fluids on sperm motility** (A) The effects
912 of secretions from the prostate and seminal vesicles on sperm motility were directly compared.
913 (B-F) The effects of secretions from the prostate (Pros) or seminal vesicles (SV) on the motility
914 parameters of epididymal sperm were tested: (B) Motile, (C) Progressive motile, (D) Curvi-
915 Linear Velocity; VCL, (E) Straight-Line Velocity; VSL and (F) Linearity; LIN is the ratio of VSL

916 to VCL of sperm that was incubated with the mixture of seminal vesicle secretions or prostate
917 extracts. (G) Viscosity of a solution containing prostate or seminal vesicle secretion with a protein
918 concentration of 10 mg/mL. (H) Experimental design to evaluate the effect of seminal vesicle
919 secretions collected from male mice treated with or without flutamide (50 mg/kg subcutaneously
920 every day for 7 days) on sperm. Note that the donor mice for sperm and seminal vesicle secretions
921 were different. (I-L) Performed bioassay using seminal vesicle fluid after treatment with vehicle
922 (Ctrl) or flutamide: (I) Motile, (J) Progressive motile, (K) LIN, (L) VSL. (M) The high
923 mitochondrial membrane potential (hMMP) was checked by the JC-1 kit. Antimycin (Anti) was
924 used as the negative control for hMMP. Data are mean ± SEM. n=3-9 independent replicates. The
925 viscosity measurement data were from n=3 repeated experiments using pooled prostate or seminal
926 vesicle extracts from at least 20 mice. Percentage data were subjected to arcsine transformation
927 before statistical analysis. (B-G, I-L) Significance was tested in comparison using Student's t-test.
928 (M) Since the results of the Bartlett test were significant, a two-way ANOVA using a generalized
929 linear model was performed. Both the flutamide administration and antimycin addition were
930 significant. The interaction was not significant. Games-Howell was performed as a post hoc test.
931 Different letters represent significantly different groups.
932
933
934

935 **Fig.2**

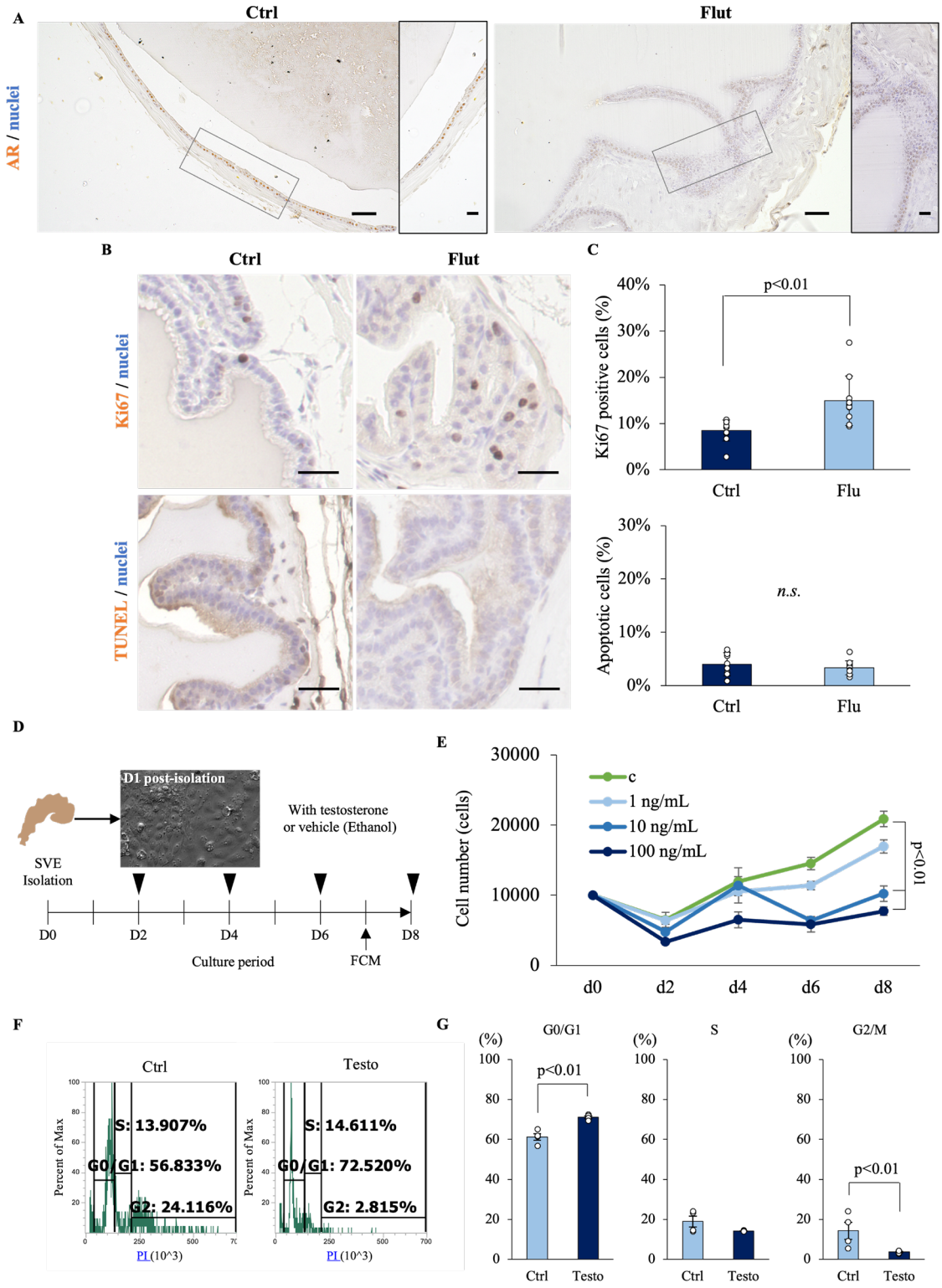

936

937

938 **Figure 2. The testosterone-androgen receptor pathway inhibits the cell proliferation of**
939 **seminal vesicle epithelial cells.** (A) The localization of the androgen receptor (AR; NR3C4) in
940 seminal vesicle of control (Ctrl) mice and those treated with flutamide (Fult). Scale bar=50 μm
941 from 10× magnification for left panel and 20 μm from 20× magnification for right panel in each
942 group. (B,C) Cell proliferation and apoptosis in seminal vesicle of control (Ctrl) mice and those
943 treated with flutamide (Fult): (B) Representative images of Ctrl and Flut staining for Ki67 (top)
944 and TUNEL (bottom). Scale bar=20 μm. (C) Percentage of Ki67 positive cells (top) and TUNEL
945 positive (bottom) in Ctrl and Flut-treated seminal vesicle sections. (D) Experimental design to
946 evaluate the effects of testosterone on the proliferation of seminal vesicle epithelial cells *in vitro*.
947 The epithelial cells were culutured with or without testosterone for 8 days. (E) Growth curves of
948 seminal vesicle epithelial cells that cultured with 0 (c), 1, 10 and 100 ng/mL of testosterone. (F,G)
949 Cell cycle status was determined by flow cytometry. Data are mean ± SEM. n=3-5 mice or
950 independent replicates. Each replicate experiments with 3-6 wells containing pooled cells from
951 3-5 mice. Percentage data were subjected to arcsine transformation before statistical analysis.
952 Significance was tested in comparison to Ctrl using Student's t-test. The cell number data at d8
953 was compared with the control using Dunnett's test.
954
955

956 **Fig.3**

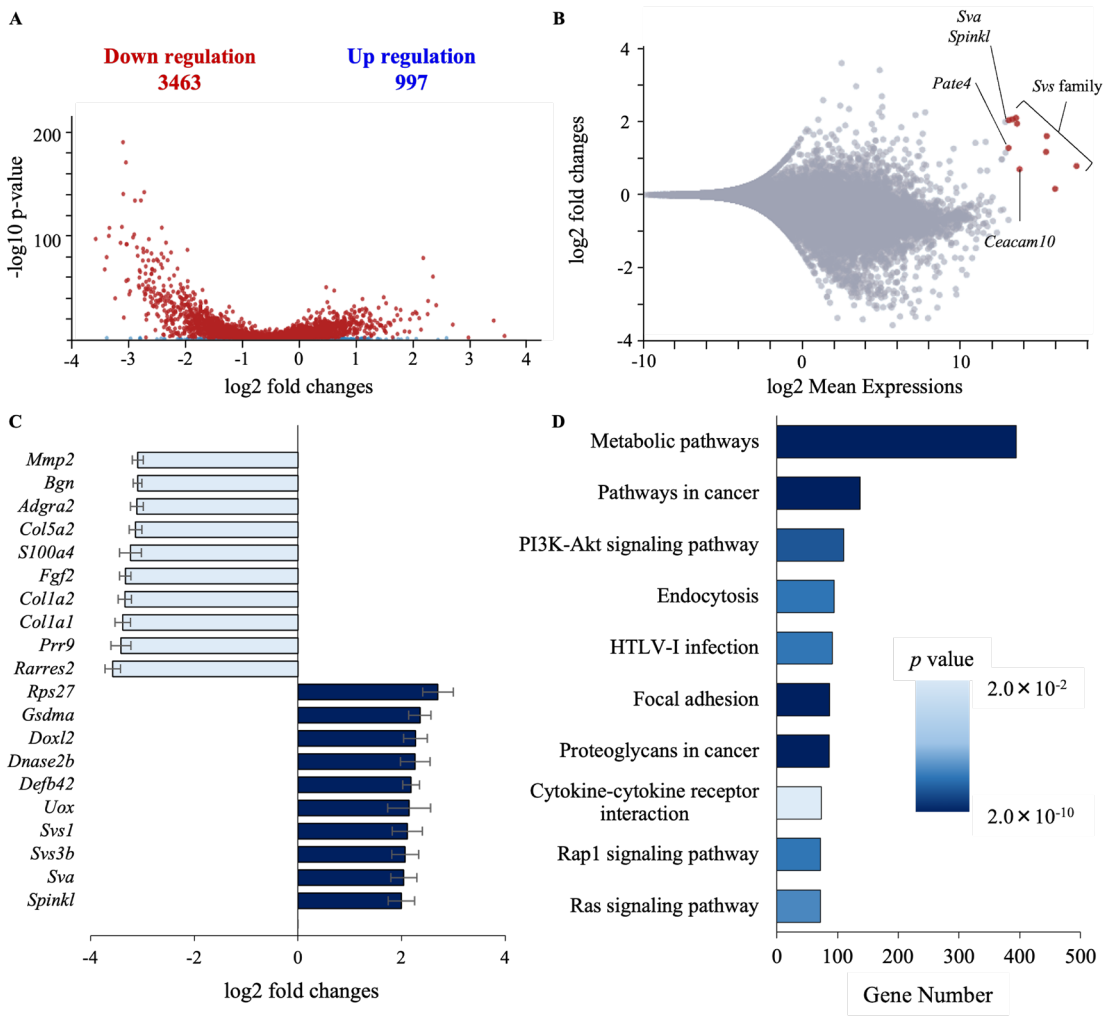

957

958 **Figure 3. Testosterone changes the expression of genes involved in metabolic pathway in**
959 **seminal vesicle epithelial cells.** (A) Volcano plot of differentially expressed genes. RNA
960 sequencing was performed using RNA extracted from the seminal vesicle epithelial cells cultured
961 with or without 100 ng/mL testosterone. Genes with a significant expression change are
962 highlighted as red dots. It found 4460 significant genes for a cutoff of P<0.05. (B) MA plot of
963 differential expression results. The seminal vesicle specific genes are highlighted as red dots
964 rather than significant genes. (C) Top 10 genes upregulated or downregulated by testosterone,
965 respectively, for altered gene expression. (D) Conducted KEGG analysis to identify differences
966 in pathway enrichment by testosterone, identifying the most variability in metabolic pathway
967 genes. It shows the number of differential expressed genes annotated to Gene Ontology shows (x

axis). p-value which measure the statistical significance of a possible functional enrichment for each term.

971 **Fig.4**

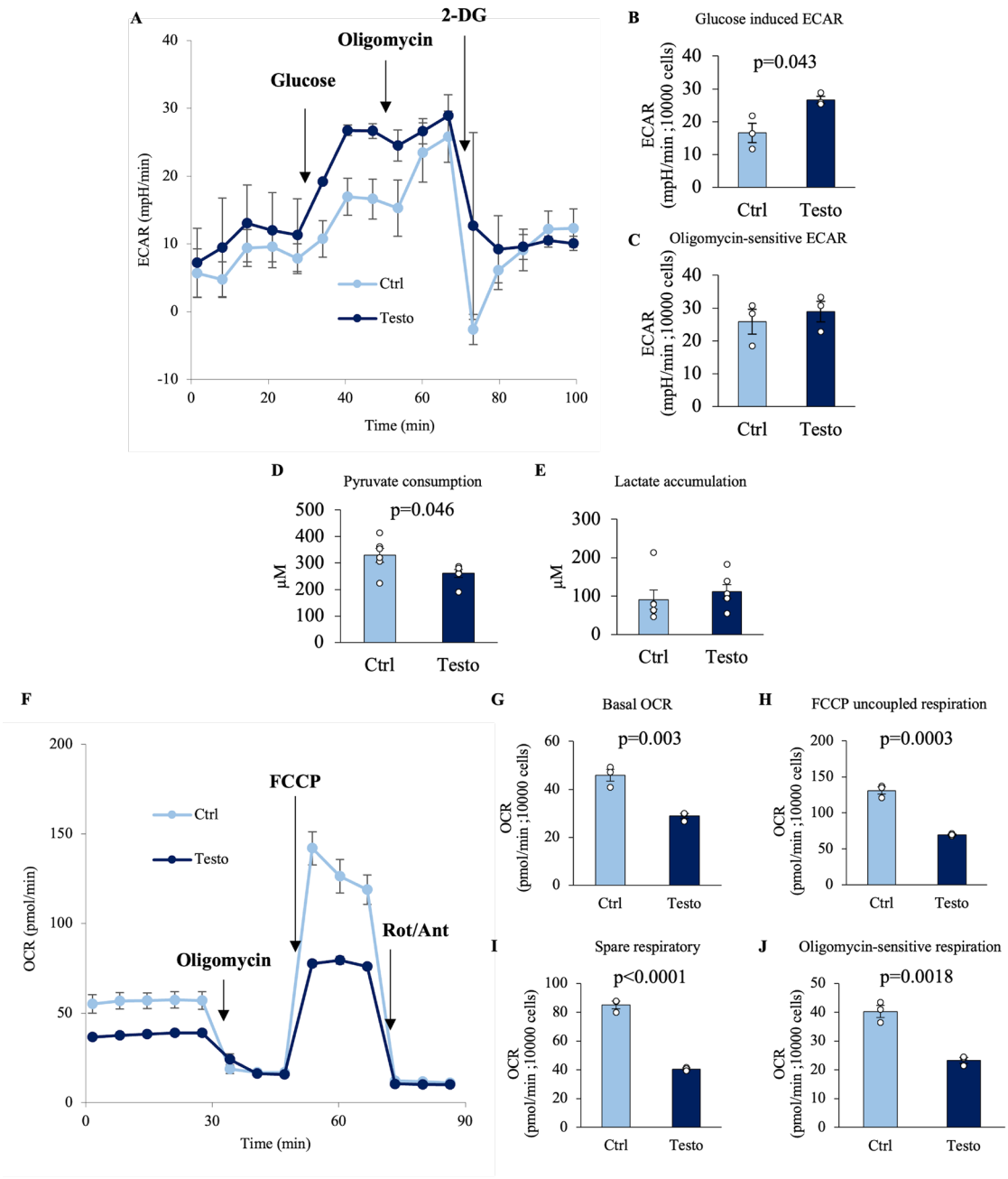

972

973 **Figure 4. Testosterone regulates glucose metabolism and mitochondrial ATP production in**
974 **seminal vesicle epithelial cells.** (A-C) Extracellular acidification rate (ECAR) analysis by an
975 extracellular flux analyzer in seminal vesicle epithelial cells cultured with 100 ng/mL
976 testosterone (Testo) or vehicle (Ctrl) for 7 days: (A) ECAR kinetics of seminal vesicle epithelial
977 cells using an extracellular flux analyzer. (B) Glucose induced ECAR and (C) Oligomycin-
978 sensitive ECAR. (D,E) The concentrations of pyruvate and lactate in the culture supernatant.

979 These measurements were normalized based on cell count and viability. (D) Pyruvate
980 concentration in the medium where seminal vesicle epithelial cells were cultured with or
981 without testosterone for 24 hours. (E) Lactate concentration. (F-J) Mitochondrial respiration
982 measurement by an extracellular flux analyzer: (F) Oxygen consumption rate (OCR) kinetics of
983 seminal vesicle epithelial cells with or without 100 ng/mL testosterone. (G) Basal OCR, (H)
984 FCCP uncoupled respiration, (I) Spare respiratory capacity and (J) Oligomycin-sensitive
985 respiration. Data are mean ± SEM of n = 3 replicate experiments with 3-6 wells containing
986 pooled cells from 3-5 mice or medium. Student's t-test was used to compare Ctrl and Testo. The
987 cells were normalized to 10,000 viable cells/well immediately before analysis. The viability of
988 the cells before experiments was 86-93%.
989

990 **Fig.5**

991 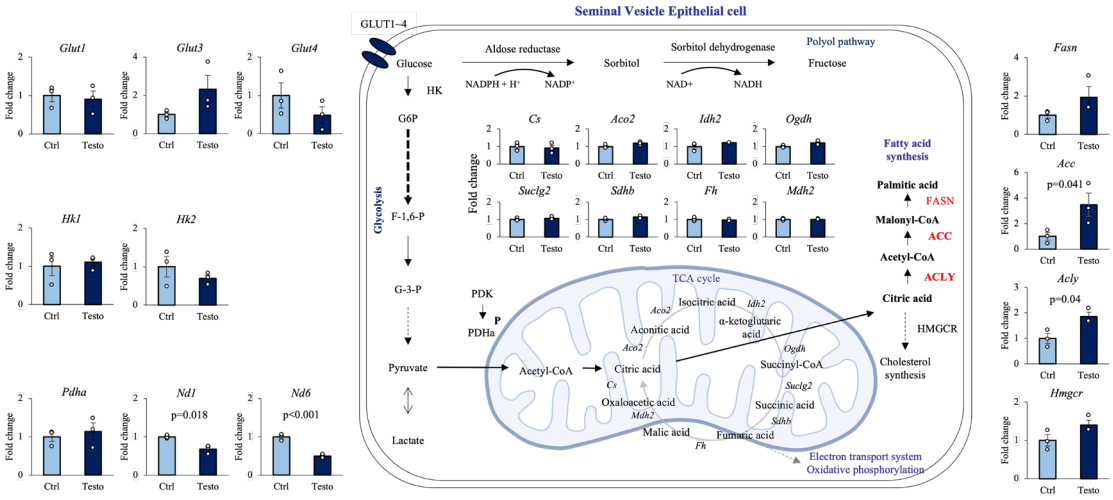

992 **Figure 5. Effect of testosterone on gene expression of enzymes involved in the glucose**
993 **metabolic pathway in seminal vesicle epithelial cells.** To elucidate the effects of testosterone
994 on gene expression of enzymes involved in glucose catabolism and anabolism in seminal vesicle
995 epithelial cells. ctrl: 7 days of culture with vehicle. Testo: 7 days of culture with 100 ng/mL
996 testosterone. Data are mean ± SEM of n = 3 replicate experiments with 3-6 wells containing
997 pooled cells from 3-5 mice. Student's t-test was used to compare Ctrl and Testo.

998

999

1000 **Fig.6**

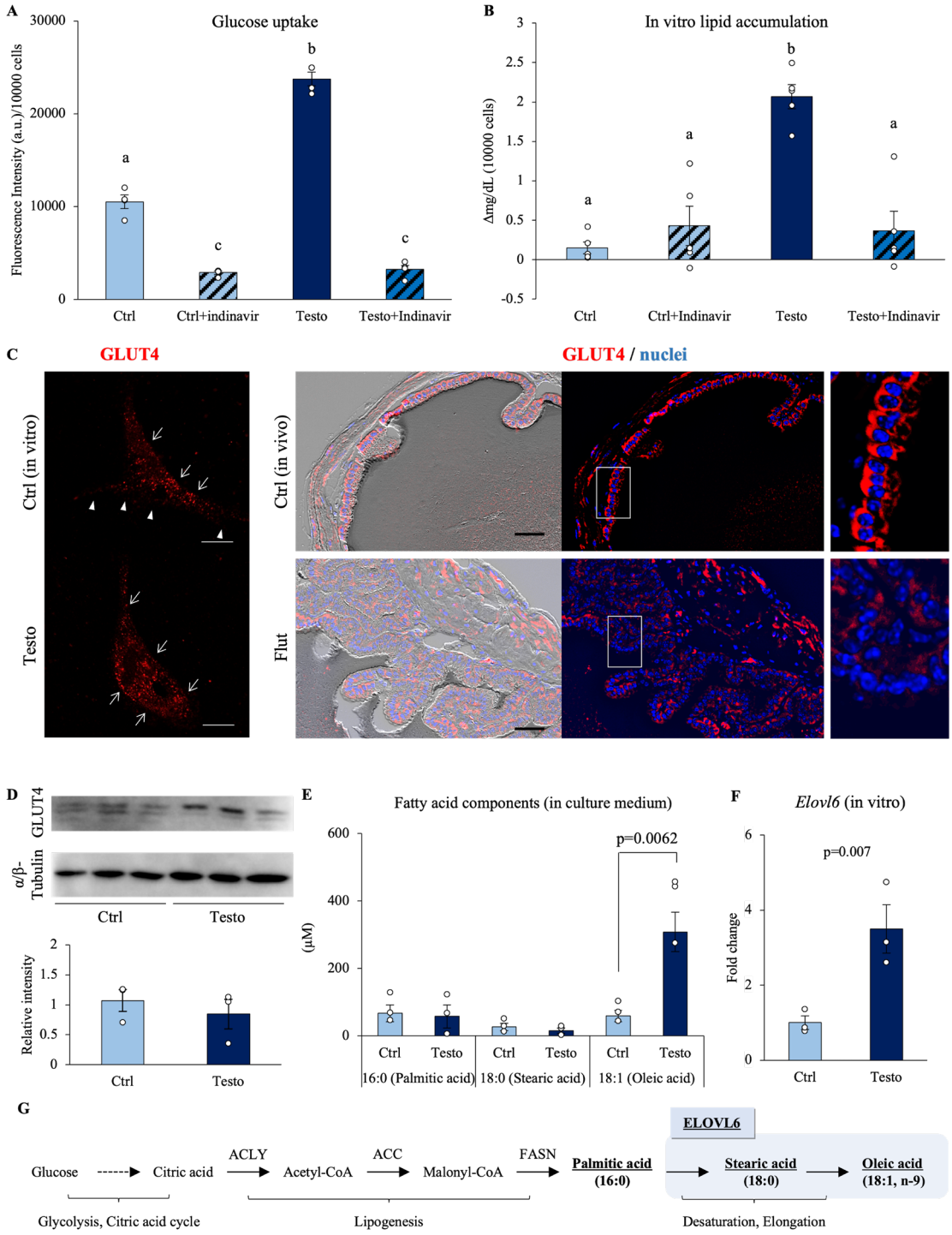

1001

1002 **Fig.6 Testosterone enhances glucose uptake and fatty acid synthesis via GLUT4 trans-**
1003 **localization in seminal vesicle epithelial cells.** (A) The glucose uptake ability of seminal vesicle
1004 epithelial cells was detected using fluorescence-tagged glucose. The cells were cultured with 100

1005 ng/mL testosterone and/or indinavir (100 μM) for 7 days and then further treated with glucose
1006 uptake probe-green for 15 min, and intracellular fluorescence was measured by flow cytometry
1007 (n=4). (B) Lipid accumulation in the medium where seminal vesicle epithelial cells were
1008 incubated for 24 hours (n=6). (C) Immunostaining of GLUT4 in flutamide-treated or vehicle mice
1009 derived seminal vesicle. Scale bar is 50 μm. (D) Western blot images of GLUT4 and α/β-tubulin
1010 in three sets of seminal vesicle epithelial cells cultured with 100 ng/mL testosterone (Testo) or in
1011 vehicle (Ctrl) for 7 days. Quantitative analysis of GLUT4 relative to α-tubulin obtained from
1012 Western blot. (E) Fatty acid composition in the medium was analyzed using gas chromatography.
1013 (F) Quantification of *Elovl* family gene expression by RT-qPCR. (G) Pathway of glucose
1014 assimilation to oleic acid. Data are mean ± SEM. n=3-6 independent replicates. Each replicate
1015 experiments with 3-6 wells containing pooled cells from 3-5 mice or medium. (A,B) The glucose
1016 uptake and lipid measurements were normalized based on cell count and viability. A two-way
1017 ANOVA was performed. Both the Indinavir and testosterone treatment were significant. The
1018 interaction was significant. Tukey's Honest Significant Difference test was performed as a post
1019 hoc test. Different letters represent significantly different groups. Student's t-test was used for
1020 comparison between the two groups.
1021
1022
1023
1024
1025
1026
1027
1028
1029

1030 **Fig.7**

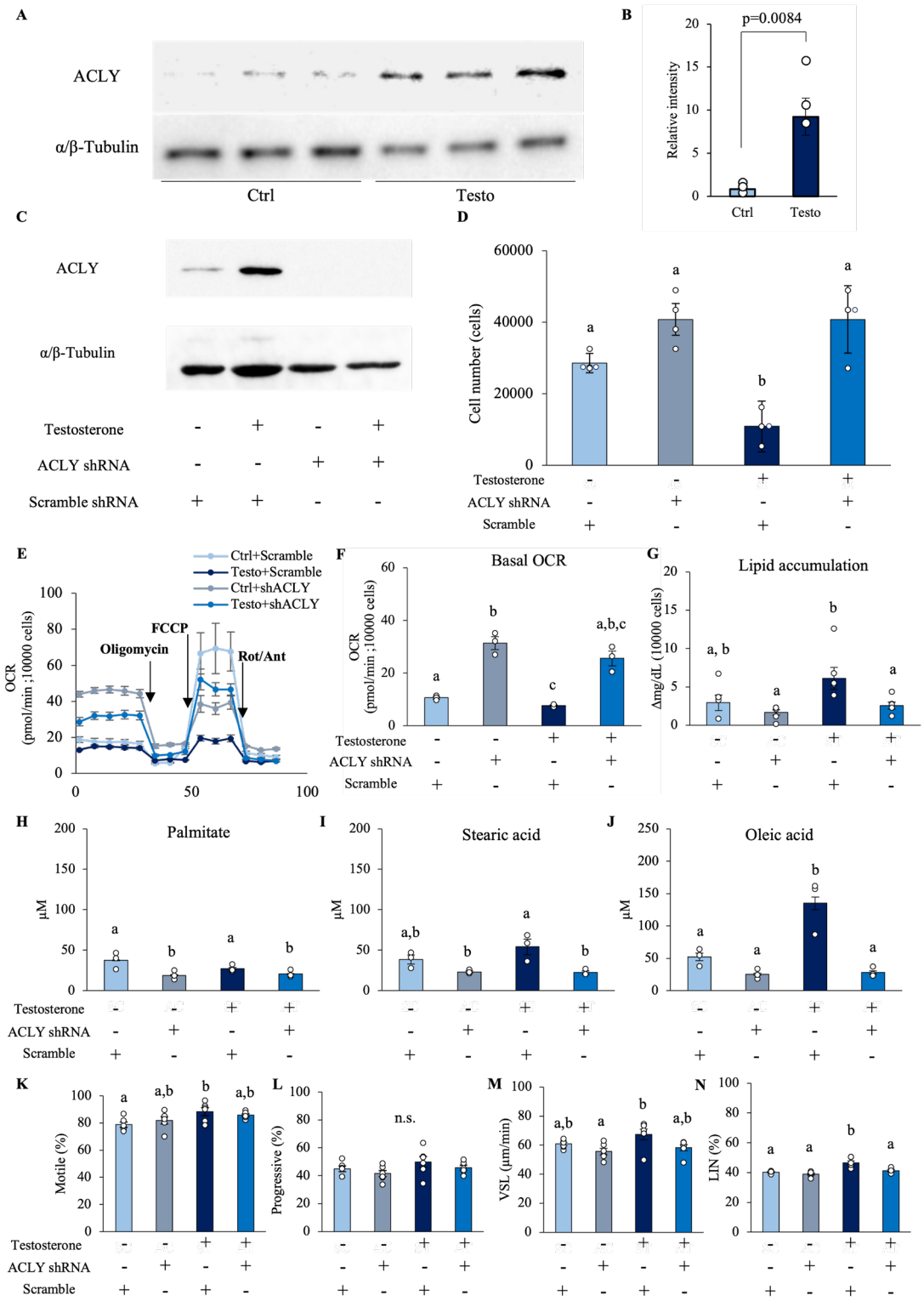

1031

1032 **Figure 7. Testosterone-regulated ACLY induces metabolic shifts in seminal vesicle epithelial**

1033 **cells.** (A) Western blot images of ACLY and α/β-tubulin in three sets of seminal vesicle epithelial

1034 cells cultured with 100 ng/mL testosterone (Testo) or in vehicle (Ctrl) for 7 days. (B) Quantitative
1035 analysis of ACLY relative to α-tubulin obtained from Western blot. (C) shRNA knockdown
1036 experiments of ACLY in seminal vesicle epithelial cells. ACLY protein levels in scrambled
1037 shRNA or ACLY shRNA-transfected seminal vesicle epithelial cells cultured with or without 100
1038 ng/mL testosterone were determined by Western blot. (D) Number of cells at 7 days after
1039 incubation. (E,F) Changes in oxygen consumption of seminal vesicle epithelial cells were
1040 analyzed by a flux analyzer: (E) Oxygen consumption rate (OCR) kinetics of seminal vesicle
1041 epithelial cells transfected with scrambled shRNA or ACLY shRNA. (F) Basal OCR. (G) The
1042 impact of ACLY knockdown on testosterone-induced fatty acid synthesis was measured. These
1043 measurements were normalized based on cell count and viability. The viability of the cells before
1044 experiments was 67-81%. (H-I) Fatty acid composition in the cultured supernatants was analyzed
1045 using gas chromatography. (H) Palmitate (C16:0). (I) Stearic acid (C18:0). (J) Oleic acid (C18:1).
1046 (K-N) The effect of culture supernatants of testosterone-treated cells on sperm motility was
1047 evaluated, especially after ACLY knockdown. (K) Motile. (L) Progressive motile. (M) Straight-
1048 Line Velocity; VSL. (N) Linearity; LIN. Data are mean ± SEM. n=3-6 independent replicates.
1049 Repeated experiments were performed with cells recovered from 3 wells containing pooled cells
1050 from 3 to 5 mice. Student's t-test was used for comparison between the two groups. Percentage
1051 data were subjected to arcsine transformation before statistical analysis. (B) Significance was
1052 tested in comparison using Student's t-test. (D,G-M) A two-way ANOVA was performed. Tukey's
1053 Honest Significant Difference test was performed as a post hoc test. (D) Both the ACLY
1054 knockdown and testosterone treatment were significant. The interaction was significant. (G) Both
1055 the ACLY knockdown and testosterone treatment were significant. The interaction was not
1056 significant. (H,I) Only the ACLY knockdown were significant. The interaction was not significant.
1057 (J) Both the ACLY knockdown and testosterone treatment were significant. The interaction was
1058 significant. (F,N) Since the results of the Bartlett test were significant, a two-way ANOVA using
1059 a generalized linear model was performed. Games-Howell was performed as a post hoc test. (E)
1060 Only the ACLY knockdown were significant. The interaction was not significant. (N)
1061 Testosterone treatment were significant. The interaction was significant. Different letters
1062 represent significantly different groups.
1063

1064 **Fig.8**

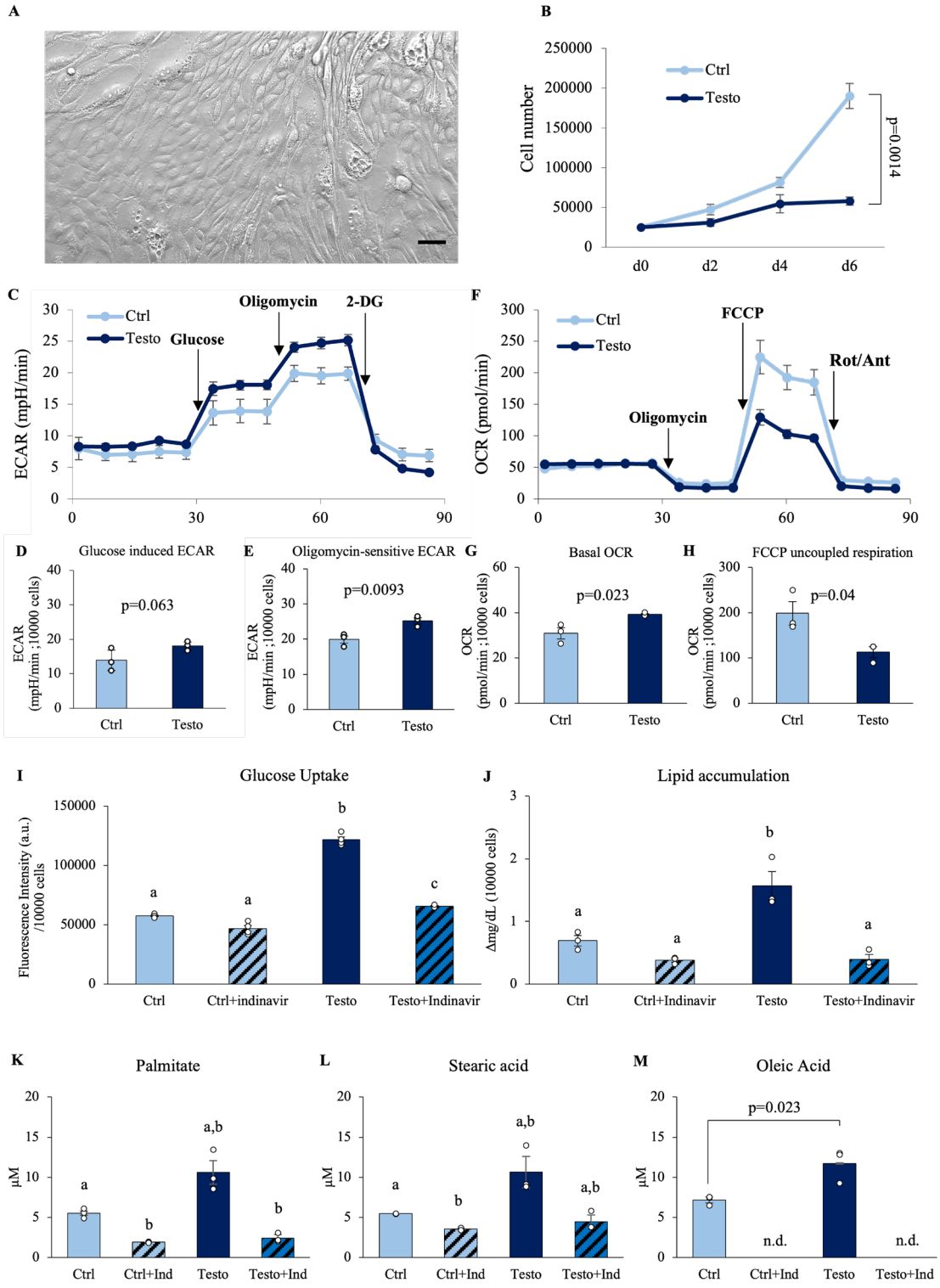

1065

1066 **Figure 8. Testosterone regulates the metabolic activity of human seminal vesicle epithelial**
1067 **cells.** (A) Representative image of human seminal vesicle epithelial cells. (B) Growth curves of

1068 seminal vesicle epithelial cells with 100 ng/mL testosterone (Testo) or without (Ctrl). (C-H)
1069 Extracellular acidification rate (ECAR) kinetics and Oxygen consumption rate (OCR) kinetics of
1070 human seminal vesicle epithelial cells after 6 days of culture with or without 100 ng/mL
1071 testosterone using a flux analyzer. (D) Glucose induced ECAR and (E) Oligomycin-sensitive
1072 ECAR. (G) Basal OCR, (H) FCCP uncoupled respiration. (I) The glucose uptake ability of
1073 seminal vesicle epithelial cells was detected using fluorescence-tagged glucose. (J) Lipid
1074 accumulation in the medium where human seminal vesicle epithelial cells were incubated for 24
1075 hours. (K-M) Fatty acid composition in the cultured supernatants was analyzed using gas
1076 chromatography. (K) Palmitate (C16:0). (L) Stearic acid (C18:0). (M) Oleic acid (C18:1). Data
1077 are mean ± SEM. n=3 independent replicates. Student's t-test was used for comparison between
1078 the two groups. (C-J) These measurements were normalized based on cell count and viability. The
1079 viability of the cells before experiments was 88-96%. (I,K,L) Since the results of the Bartlett test
1080 were significant, a two-way ANOVA using a generalized linear model was performed. Games-
1081 Howell was performed as a post hoc test. Both the Indinavir and testosterone treatment were
1082 significant. The interaction was significant. (J) A two-way ANOVA was performed. Tukey's
1083 Honest Significant Difference test was performed as a post hoc test. Both the Indinavir and
1084 testosterone treatment were significant. The interaction was significant. Different letters represent
1085 significantly different groups.
1086
1087

1088 **Fig.9**

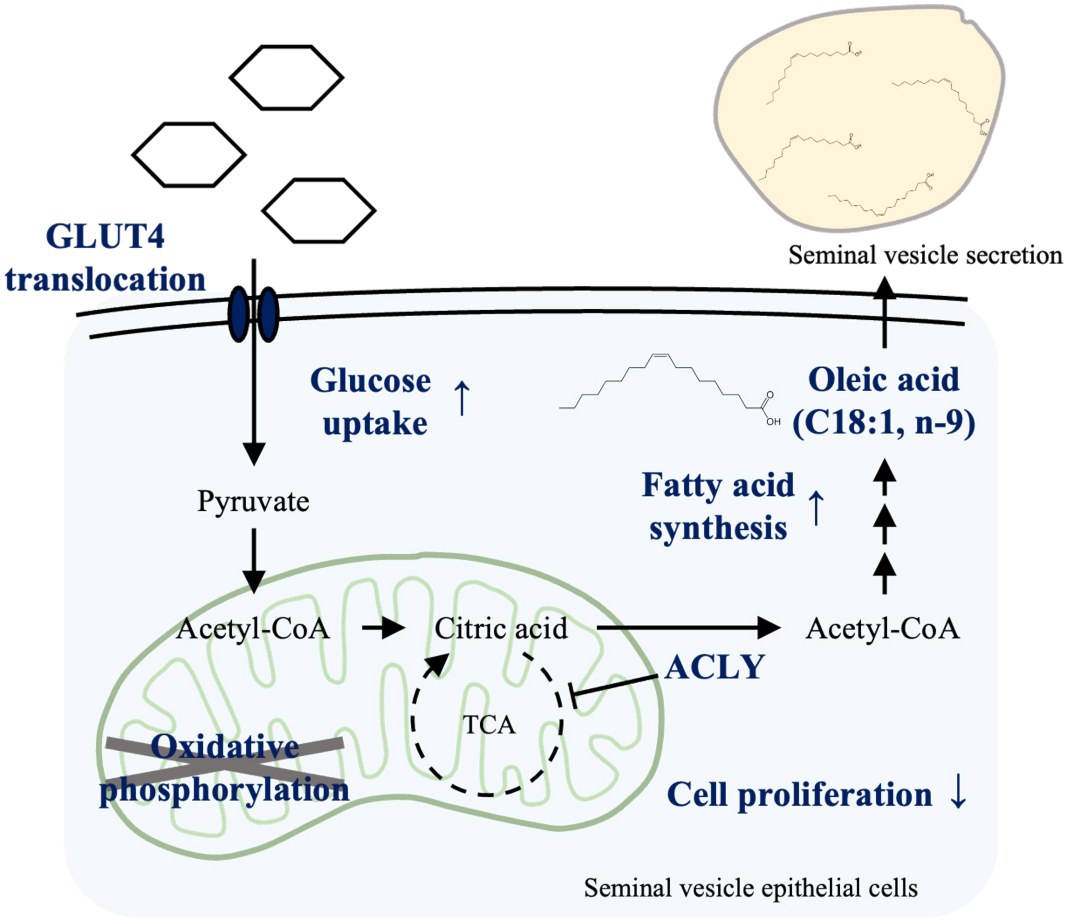

1089

1090 **Figure 9. Testosterone-induced metabolic reprogramming in seminal vesicle epithelial cells.**
1091 Testosterone promotes glucose uptake by changes in the localization of GLUT4 in seminal vesicle
1092 epithelial cells. ATP-citrate-lyase (ACLY) activated by testosterone promotes fatty acid synthesis
1093 by skipping some tricarboxylic acid (TCA) cycle steps. Simultaneously, cell proliferation in the
1094 epididymal epithelial cells is suppressed. Testosterone also promotes the synthesis of oleic acid
1095 from acetyl-CoA synthesized by ACLY.

1096

1097 **Supplemental Figure 1**

A

	Average	SEM
Motility (%)	91.5	7.5
Progressive motile (%)	57.5	6.6
VCL (μm/sec)	190.8	9.4
VSL (μm/sec)	74.7	3.5
LIN (%)	38.0	3.6
Viscosity of HTF (mPa·s)	0.8	0.01

B

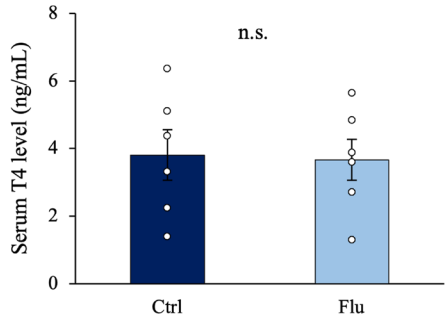

C

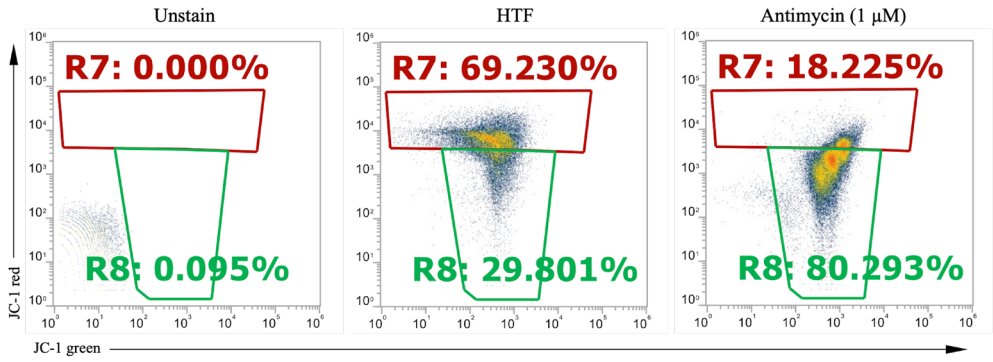

D

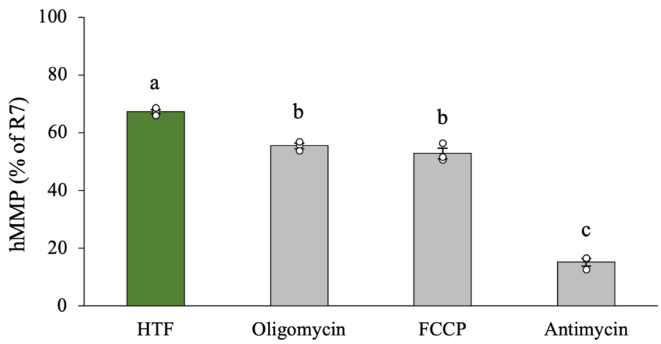

E

		No. of oocytes		
		Inseminated	Cleaved	(%)
	HTF	349	313	89.7
+SV extracts	Ctrl	86	23	26.7
	Flu	94	13	13.8

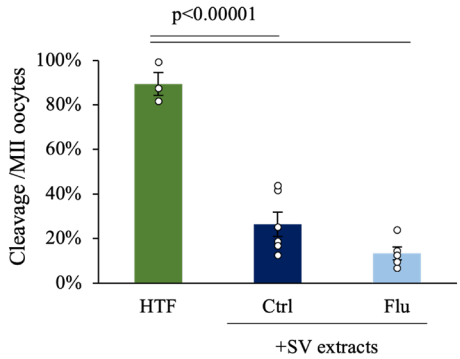

1098

1099 **Supplemental Figure 1. Sperm quality control data and exploratory research into the effects**

1100 **of seminal vesicle secretions on sperm fertilization** (A) The baseline information for the

1101 epididymal sperm used in Fig 1 and Supplemental Fig 2A. Curvi-Linear Velocity; VCL, Straight-
1102 Line Velocity; VSL and Linearity; LIN is the ratio of VSL to VCL of sperm incubated in HTF
1103 medium one hour. (B) Serum testosterone levels in seminal vesicle secretion donors. (C) Typical
1104 flow cytometry patterns for JC-1 staining From left to right: Unstained, untreated (HTF), and
1105 antimycin-treated sperm. R7 and R8 were gated to obtain positive rates of over 60% for HTF and
1106 antimycin, respectively. (D) The effect of various drugs on the proportion of high mitochondrial
1107 membrane potential (hMMP; R7). Data are mean ± SEM. At least three independent replicates.
1108 (B) Significance was tested in comparison using Student's t-test. (D) Percentage data were
1109 subjected to arcsine transformation before statistical analysis. Differences between groups were
1110 assessed by one-way analysis of variance (ANOVA). When ANOVA was significant, differences
1111 among values were analyzed by Tukey's Honest Significant Difference test for multiple
1112 comparisons. Different letters represent significantly different groups.
1113

1114 **Supplemental Figure 2**

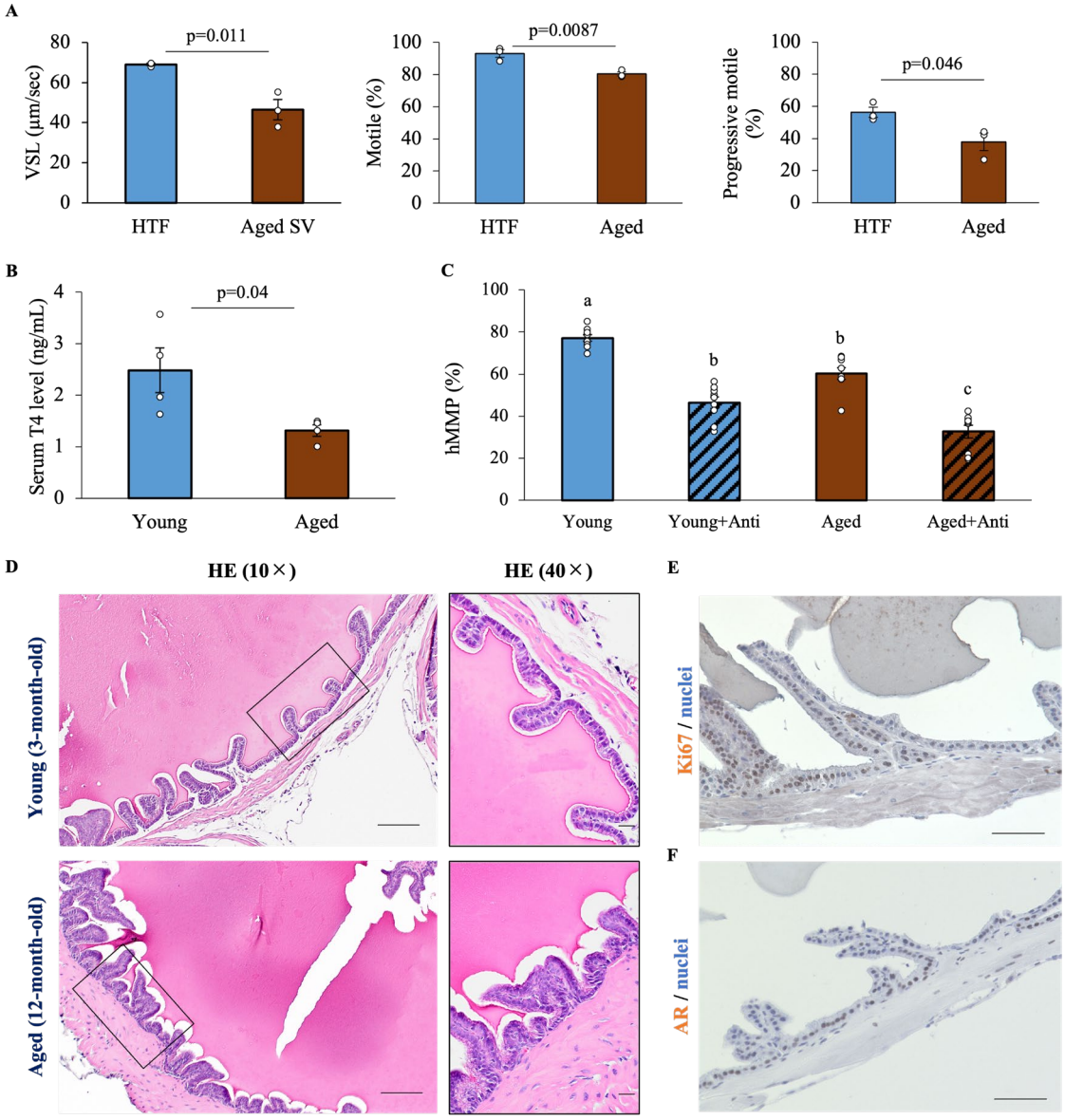

1115

1116 **Supplemental Figure 2. Characteristics of the seminal vesicle in aging mice** (A) The effects
1117 of secretions from aged seminal vesicle fluid on sperm motility. Straight-Line Velocity; VSL,
1118 Motile, and Progressive motile. (B) Serum testosterone (T4) levels in young (3 months old) or
1119 aged (12 months) mice. (C) The high mitochondrial membrane potential (hMMP) was checked
1120 by the JC-1 kit. (D) Hematoxylin/Eosin (HE) staining in seminal vesicles of young and aged
1121 mice. Scale bar=50 μm for left panel and 20 μm for right panel. (E) Representative images
1122 staining for Ki67. Scale bar=50 μm. (F) The localization of the androgen receptor (AR; NR3C4)
1123 in the seminal vesicles of aged mice. Scale bar=50 μm. (E,F) Images were obtained at 10×

magnification. Data are mean ± SEM. At least three independent replicates. Percentage data were subjected to arcsine transformation before statistical analysis. (A,B) Significance was tested in comparison using Student's t-test. (C) A two-way ANOVA was performed. Tukey's Honest Significant Difference test was performed as a post hoc test. Both the age and antimycin treatment were significant. The interaction was not significant. Different letters represent significantly different groups.

1131 **Supplemental Figure 3**

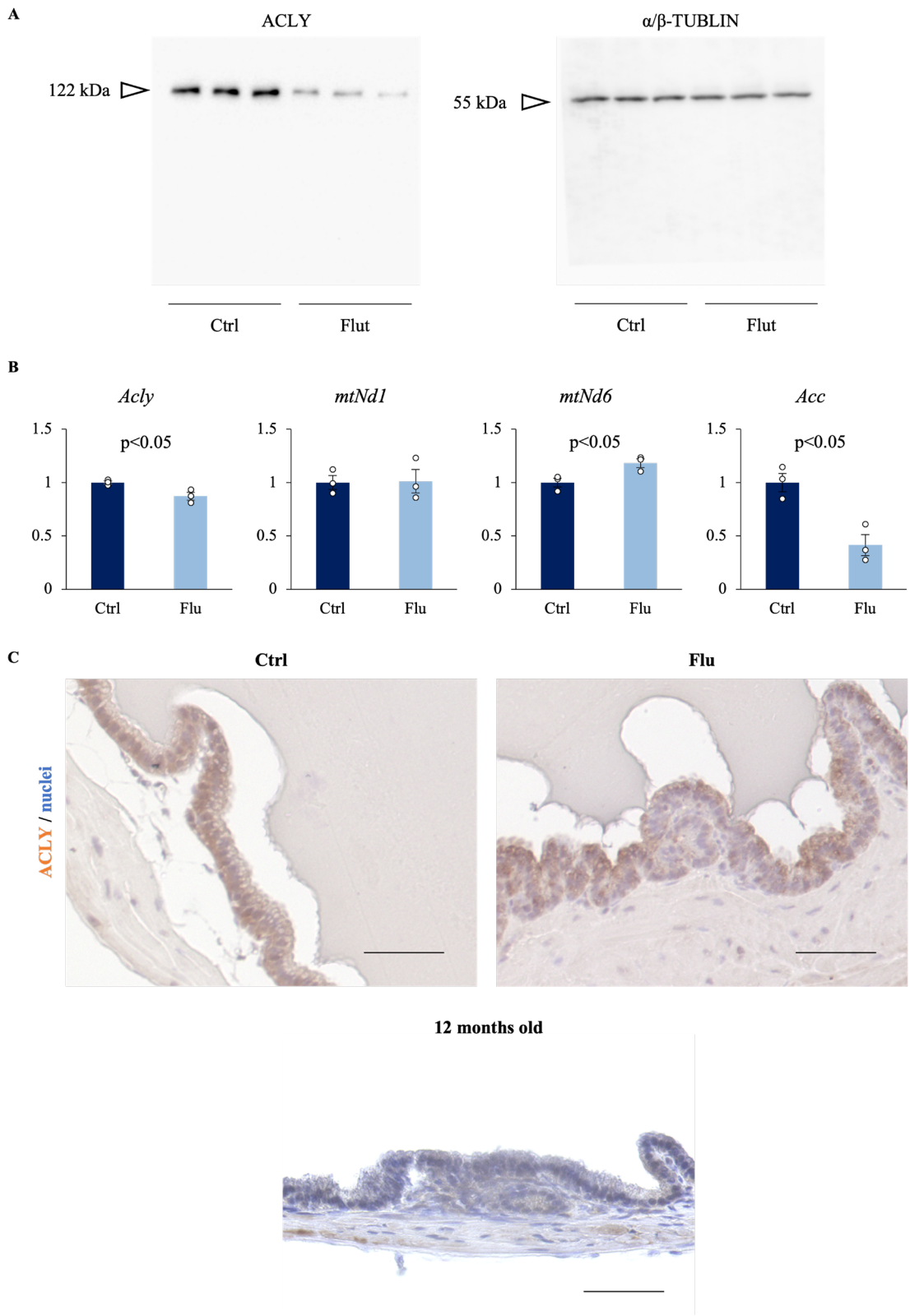

1132

1133 **Supplemental Figure 3. ACLY expression in *in vivo* seminal vesicle** (A) Representative
1134 Western blot images of ACLY and α-tubulin in three sets of seminal vesicle collected from 50
1135 mg/kg flutamide subcutaneously for 7 days (Flut) or vehicle treated mice (Ctrl). (B)
1136 Quantification of *Acly mtNd1, mtNd6 and Acc* gene expression by RT-qPCR. Data are mean ±
1137 SEM. Student's t-test was used for comparison between the two groups (n=3). (C) ACLY
1138 immunostaining: seminal vesicles from wild-type mice, flutamide-treated mice, and 12-month-
1139 old aging mice. Scale bar is 50 μm.
1140

1141 **Supplemental Figure 4**

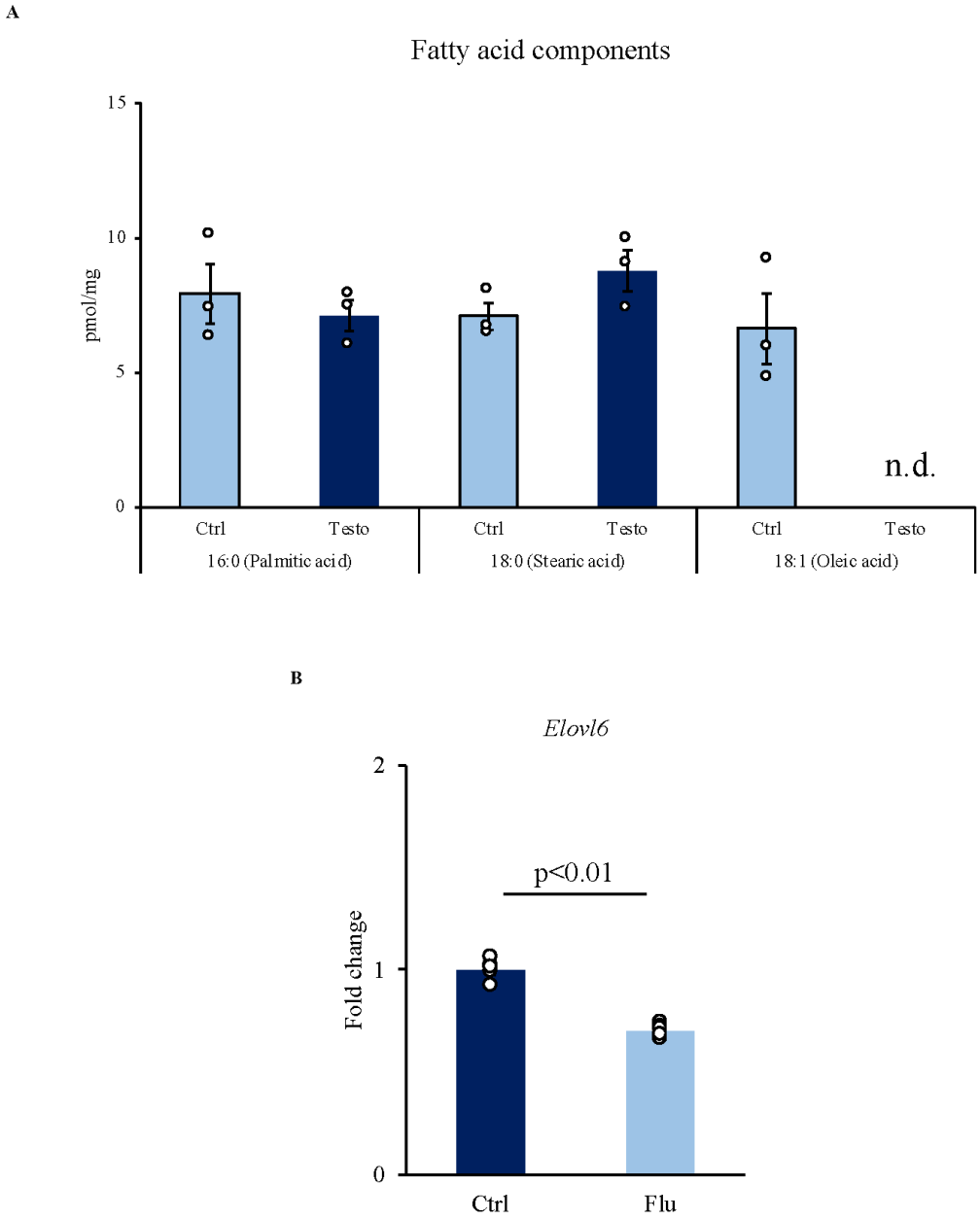

1142

1143 **Supplemental Figure 4. Oleic acid synthesis *in vivo* regulated by the testosterone-androgen**
1144 **receptor system** (A) Fatty acid composition of seminal vesicle extracts in flutamide-treated (Flu)
1145 or vehicle mice (Ctrl) pretreated with a methylation kit was analyzed by gas chromatography.
1146 *Moles contained per unit wight of seminal vesicle secretions. (B) Quantification of *Elovl6* gene
1147 expression by RT-qPCR. Data are mean ± SEM. Student's t-test was used for comparison between
1148 the two groups (n=5).

1149

Supplemental Figure 5

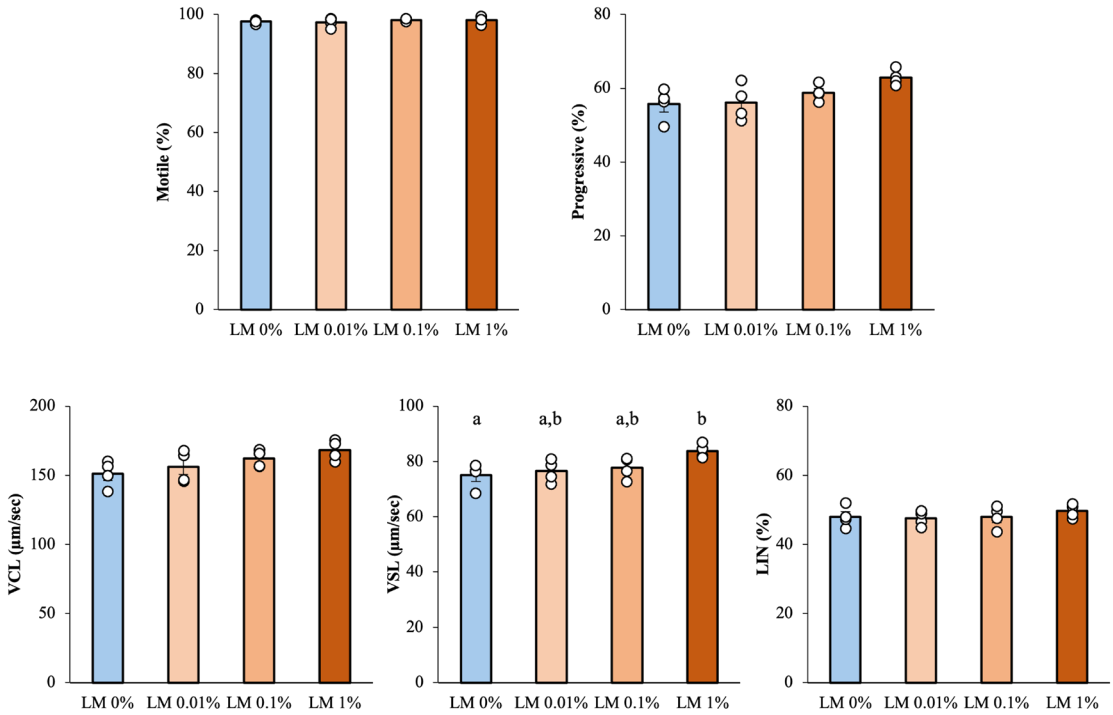

Supplemental Figure 5. The effects of lipid mixture on sperm function. The lipid mixture (LM) improves the VSL of sperm. Here, LM means that sperm were cultured in HTF medium containing a lipid mixture for 1 hour, and the control (LM 0%) means without LM. Curvi-Linear Velocity; VCL, Straight-Line Velocity; VSL and Linearity; LIN is the ratio of VSL to VCL. Data are mean ± SEM of n = 4 replicate experiments. Percentage data were subjected to arcsine transformation before statistical analysis. Differences between groups were assessed by one-way analysis of variance (ANOVA). When ANOVA was significant, differences among values were analyzed by Tukey's Honest Significant Difference test for multiple comparisons. Different letters represent significantly different groups.

1163 **Supplemental Figure 6**

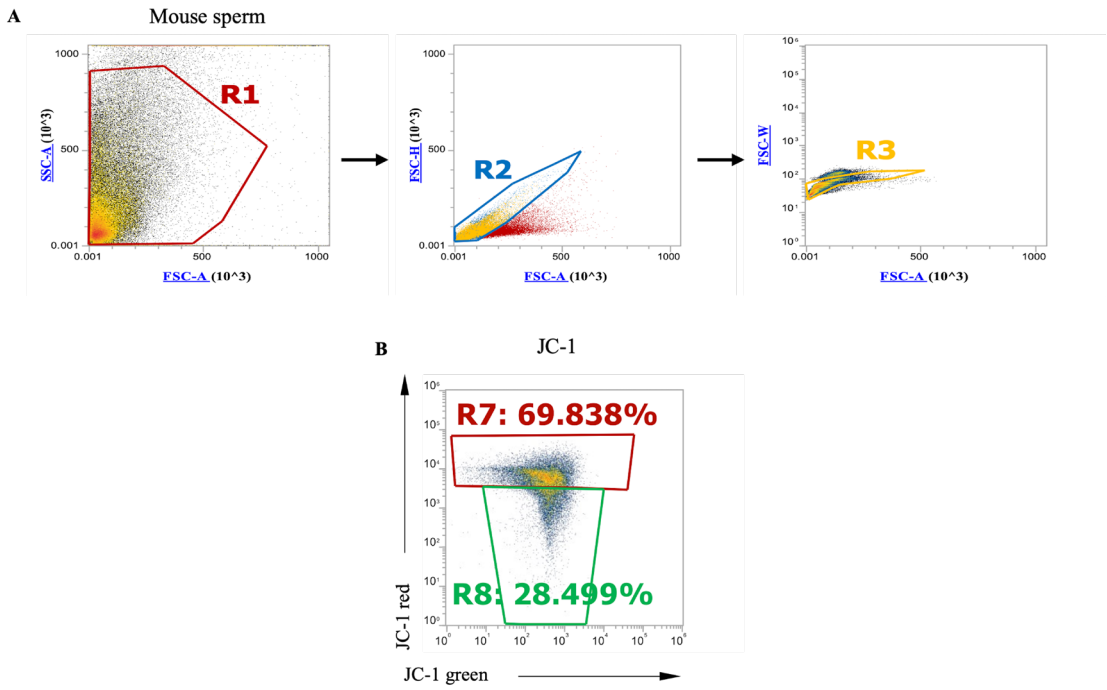

1164

1165 **Supplemental Figure 6. Gating strategy of flow cytometry for sperm** (A) Gating strategy for
1166 the selection of single sperm. Using forward scatter (FSC)-A and side scatter (SSC)-A dot plots,
1167 similar size and complexity cells were firstly selected (R1). In FSC-A and FSC-H dot plots and
1168 FSC-A and FSC-W dot plots, similar-size cells were accumulated near area; thus, using these
1169 plots, again similar-size cells were selected (R2, R3). The cells in R3 were used for below
1170 analysis. (B) The dot plots of 5,5’,6,6’-tetrachloro-1,1’,3,3’-tetraethylbenzimidazolyl
1171 carbocyanine iodide (JC-1) green (x-axis) and red (y-axis). The percentage of JC-1 red-positive
1172 sperm (R7) was used for the analysis.

1173

1174 **Supplemental Figure 7**

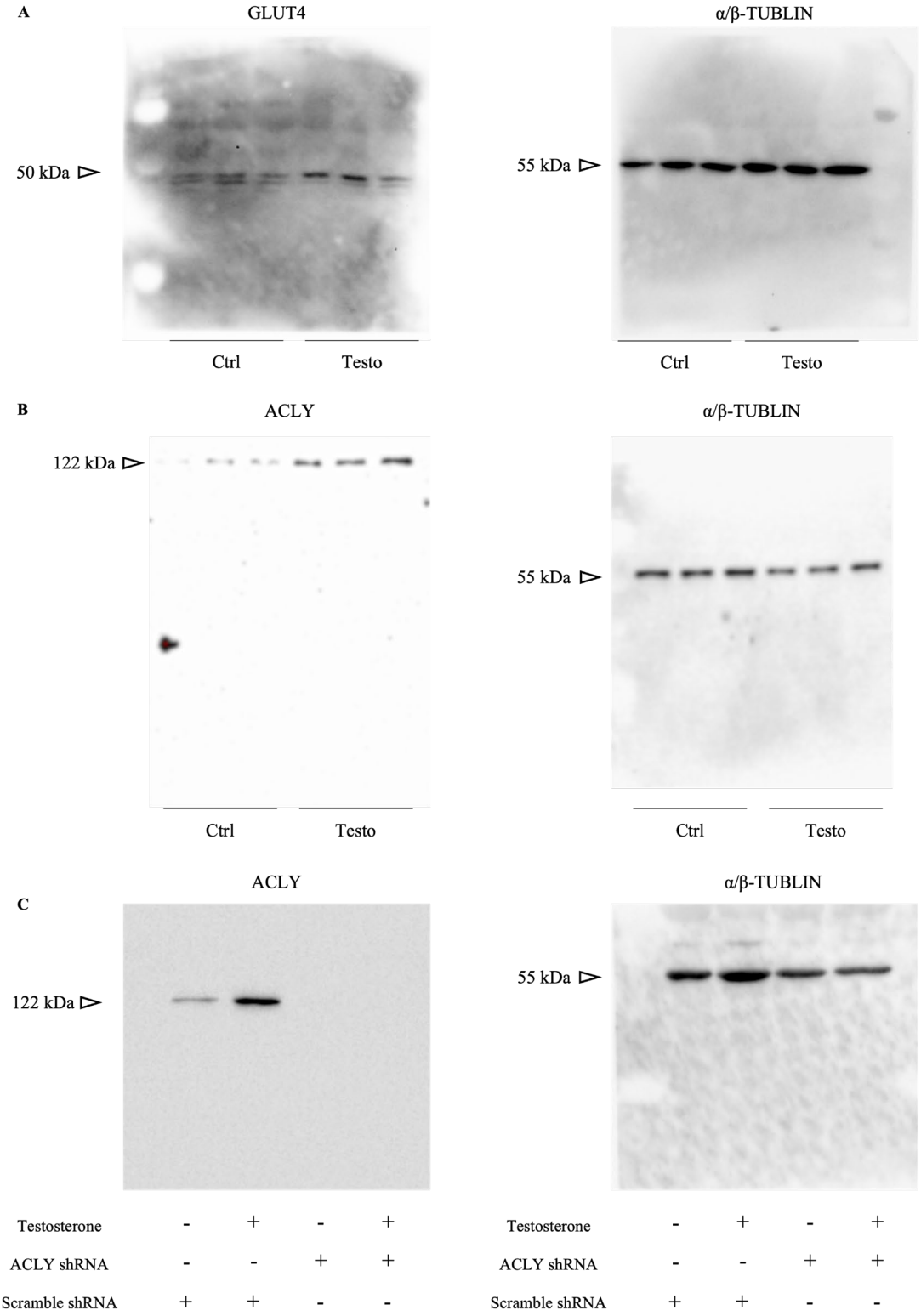

1175

1176 **Supplemental Figure 7. Full-length blotting images of western blotting** (A) Full-length

1177 blotting images of GLUT4 and α/β-TUBLIN in seminal vesicle epithelial cells cultured with

1178 100 ng/mL testosterone (Testo) or in vehicle (Ctrl) in Figure 6D. (B) Full-length blotting images
1179 of ACLY and α/β-TUBLIN in seminal vesicle epithelial cells cultured with 100 ng/mL
1180 testosterone (Testo) or in vehicle (Ctrl) in Figure 8A. (C) Full-length blotting images of ACLY
1181 and α/β-TUBLIN in seminal vesicle epithelial cells in Figure 8C. ACLY protein levels in
1182 scrambled shRNA or ACLY shRNA-transfected seminal vesicle epithelial cells cultured with or
1183 without 100 ng/mL testosterone were determined by Western blot.
1184

1185 **Supplemental Figure 8**

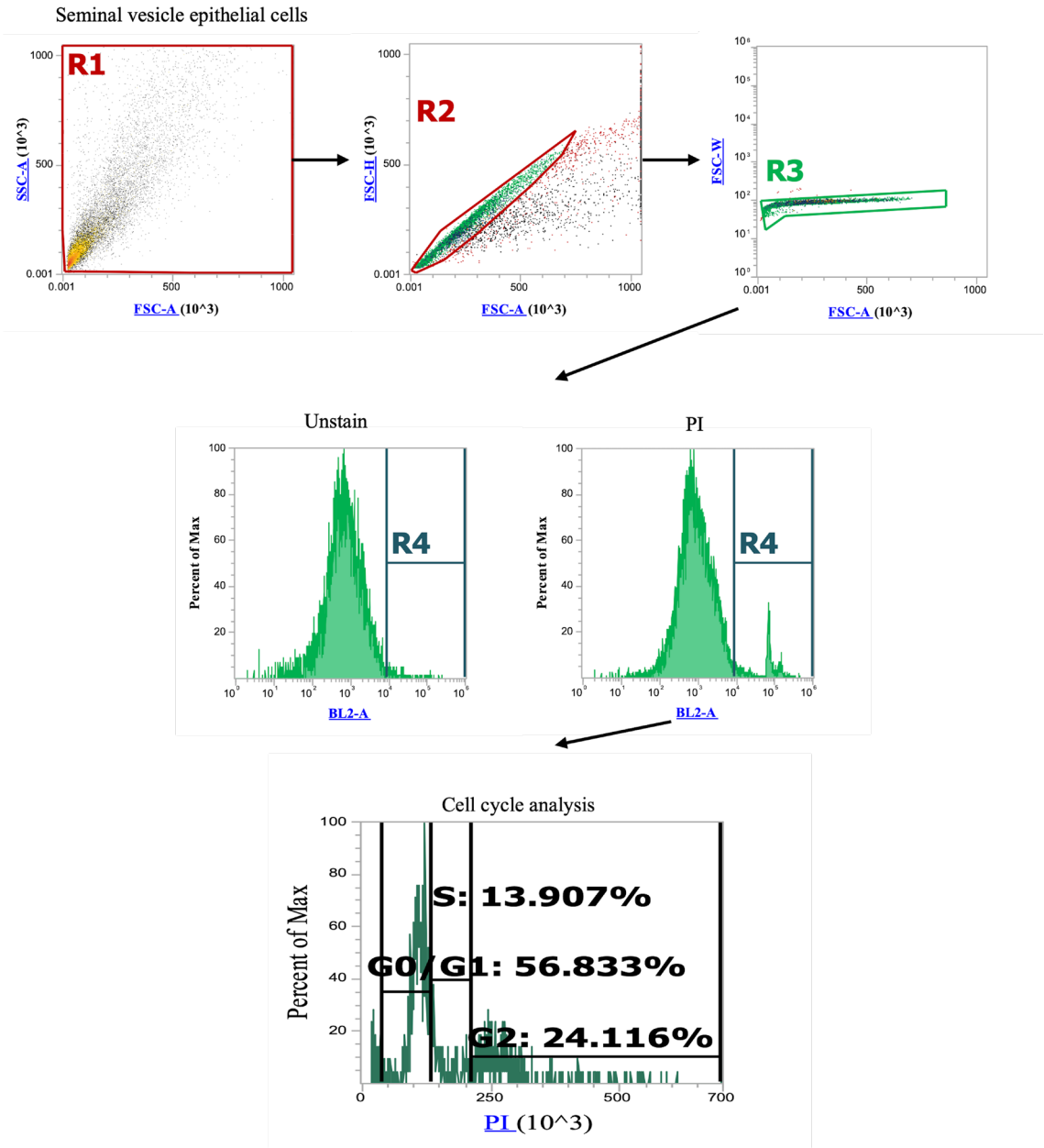

1186

1187 **Supplemental Figure 8. Gating strategy of flow cytometry for seminal vesicle epithelial cells**
1188 Gating strategy for the selection of single sperm. Using forward scatter (FSC)-A and side scatter
1189 (SSC)-A dot plots, similar size and complexity cells were firstly selected (R1). In FSC-A and
1190 FSC-H dot plots and FSC-A and FSC-W dot plots, similar-size cells were accumulated near area;
1191 thus, using these plots, again similar-size cells were selected (R2, R3). The cells in R3 were
1192 applied to the propidium iodide (PI) histogram plot. Labelling DNA with PI allows fluorescence-
1193 based analysis of the cell cycle. The intensity of PI fluorescence correlates with the amount of

1194 DNA in each cell. Comparing the G1 and G2 phases, the amount of DNA doubles in the G2 phase,
1195 so the fluorescence intensity of the cell population also doubles.
1196
1197

Table S1. Primer sequences used for quantitative real-time PCR.

Gene	Forward primer (5'→3')	Reverse primer (5'→3')
Acc	GCCTCTTCCTGACAAACGAG	TGACTGCCGAAACATCTCTG
Acly	AGGTCTCTCTGCAGCCATGT	AAGCTTTCCTCGACGTTTGA
Aco2	CTAGCCTCAGCCCAGTGAAC	CCTTCAGCCACCAGTGAAAT
Cs	CAGATGCCCACAGAGGAACA	AGCTTGGCAATGAGGTCCAT
ElovI6	CCCGAACTAGGTGACACGAT	CCGCAAGGCGTAGTAAGAGT
Fasn	AGCACACATCCTAGGCATCC	TGTCGTGTCAGTAGCCGAGT
Fh	AGCAATGCATATTGCTGCTG	CGCATACTGGACTTGCTGAA
Glut1	AAACATGGAACCACCGCTAC	AGGCCAACAGGTTCATCATC
Glut2	GCCTGTGTATGCAACCATTG	TGGCCCAATCTCAAAGAAAC
Glut3	TGTCACAGGAGAAGCAGGTG	GCTCCAATCGTGGCATAGAT
Glut4	ACTCTTGCCACACAGGCTCT	AATGGAGACTGATGCGCTCT
Hk1	TATCGGTCCAGCACGTATGC	ACATCGTGACCCACACAGTC
Hk2	GGGTAGCCACGGAGTACAAA	TGGATTGAAAGCCAACTTCC
Hmgcr	TGGAGATCATGTGCTGCTTC	GCGACTATGAGCGTGAACAA
Idh2	CCGTCTTCAGAGAGCCAATC	GAAATGGACTCGTCGGTGTT
Mdh2	GCTTTGTCTTCTCCCTCGTG	CAAAGTCCTCGCCTTTCTTG
Nd1	CAGGATGAGCCTCAAACTCC	CCGGTTTGTTTCTGCTAGGG
Nd6	GGTTGGTTGTCTTGGGTTAGC	TAGATCCCCAAGTCTCTGGA
Ogdh	ACATGGCACAGTGCATCATT	ACATCTGCAGAAACCGCTCT
Pdha	GGGGACGTCTGTTGAGAGAG	TGTGTCCATGGTAGCGGTAA
Sdhb	ACTGGTGGAACGGAGACAAG	GTTAAGCCAATGCTCGCTTC
Suclg2	CTTTGGTGGGATCGTCAACT	AACAGCTTTCTTGGCTGCAT
L19	GGCATAGGGAAGAGGAAGG	GGATGTGCTCCATGAGGATGC

1198